



Delft University of Technology

## From flat sheets to curved geometries

### Origami and kirigami approaches

Callens, Sebastien; Zadpoor, Amir A.

#### DOI

[10.1016/j.mattod.2017.10.004](https://doi.org/10.1016/j.mattod.2017.10.004)

#### Publication date

2017

#### Document Version

Final published version

#### Published in

Materials Today

#### Citation (APA)

Callens, S., & Zadpoor, A. A. (2017). From flat sheets to curved geometries: Origami and kirigami approaches. *Materials Today, 21* (April 2018)(3), 241-264. <https://doi.org/10.1016/j.mattod.2017.10.004>

#### Important note

To cite this publication, please use the final published version (if applicable).  
Please check the document version above.

#### Copyright

Other than for strictly personal use, it is not permitted to download, forward or distribute the text or part of it, without the consent of the author(s) and/or copyright holder(s), unless the work is under an open content license such as Creative Commons.

#### Takedown policy

Please contact us and provide details if you believe this document breaches copyrights.  
We will remove access to the work immediately and investigate your claim.



# From flat sheets to curved geometries: Origami and kirigami approaches

Sebastien J.P. Callens\*, Amir A. Zadpoor

Department of Biomechanical Engineering, Delft University of Technology (TU Delft), Mekelweg 2, Delft 2628CD, The Netherlands

Transforming flat sheets into three-dimensional structures has emerged as an exciting manufacturing paradigm on a broad range of length scales. Among other advantages, this technique permits the use of functionality-inducing planar processes on flat starting materials, which after shape-shifting, result in a unique combination of macro-scale geometry and surface topography. Fabricating arbitrarily complex three-dimensional geometries requires the ability to change the intrinsic curvature of initially flat structures, while simultaneously limiting material distortion to not disturb the surface features. The centuries-old art forms of origami and kirigami could offer elegant solutions, involving origami folding and cutting to transform flat papers into complex geometries. Although such techniques are limited by an inherent developability constraint, the rational design of the crease and cut patterns enables the shape-shifting of (nearly) inextensible sheets into geometries with *apparent* intrinsic curvature. Here, we review recent origami and kirigami techniques that can be used for this purpose, discuss their underlying mechanisms, and create physical models to demonstrate and compare their feasibility. Moreover, we highlight practical aspects that are relevant in the development of advanced materials with these techniques. Finally, we provide an outlook on future applications that could benefit from origami and kirigami to create intrinsically curved surfaces.

## Introduction

The many developments in additive manufacturing (AM) over the last decades have significantly increased the attractiveness of this manufacturing technique to fabricate arbitrarily complex three-dimensional (3D) geometries at the nano-, micro-, and macro-scales. Examples include bone-substituting biomaterials [1], penta-mode mechanical metamaterials [2,3], triply periodic minimal surfaces [4], and energy-absorbing cellular architectures [5]. Despite many advantages of AM, one major limitation is the incompatibility with planar surface patterning and imprinting processes, which are crucial for imbuing surfaces with specific functionalities such as hydro- or oleophobicity [6], integration of electronic circuits [7], or control over cell interaction in the case of biomaterials [8]. The ability to combine arbitrarily com-

plex surface features with arbitrarily complex geometries could enable development of advanced materials with an unprecedented set of functionalities.

A potential solution to this deadlock is provided by another manufacturing paradigm, which has been of growing interest to the scientific community during recent years: the shape-shifting of thin, planar sheets (which we consider 2D) into complex structures [9–12]. The planar sheets could first be decorated using planar patterning processes, after which they are transformed into complex 3D geometries. Additional advantages are the efficient and inexpensive production methods of the 2D sheets and their efficient packing for storage and transportation [11,13]. Moreover, the 2D-to-3D paradigm is particularly interesting for the development of micro- or nanoscale 3D constructs (e.g. micro- and nanoelectromechanical devices [14]) since conventional macroscale techniques cannot easily be scaled down to allow fabrication of such small structures [15,16]. As such, the out-of-plane transformation of 2D sheets opens up new opportunities

\* Corresponding author.

E-mail address: Callens, S.J.P. (s.j.p.callens@tudelft.nl).





for the development of complex 3D structures with functionalized surfaces, especially at small length scales.

An important parameter governing the complexity of 3D structures is the surface curvature and the variation thereof throughout the structure. In order to create arbitrarily complex 3D structures from 2D sheets, the curvature of the initially flat sheets should be altered in a controllable manner. The simplest curved shapes could be obtained through bending or rolling of flat sheets. However, more complex target shapes are characterized by “double curvature” and exhibit spherical (dome-shaped) or hyperbolic (saddle-shaped) geometries, which cannot be realized with inextensional deformations of a flat sheet (this is readily understood when attempting to wrap a sphere or saddle with paper). Instead, the flat sheet would need to be subjected to in-plane distortions in order to achieve double-curved parts. At the macro-scale, for example, flat sheet-metal is plastically stretched to create double-curved shells (e.g. using (multi-point) stretch-forming [17]), and fiber-reinforced composite laminates are subjected to in-plane shearing deformations [18]. At smaller scales, researchers have recently used stimulus-responsive materials that exhibit in-plane distortions in the form of differential shrinkage [13,19] or swelling [20,21] to achieve complex curved shapes from initially flat sheets, which is closely related to non-uniform growth processes in initially planar shapes observed in nature, resulting in wavy patterns at the edges of plant leaves [22,23] and enabling the blooming of the lily flower [24].

Subjecting 2D sheets to in-plane distortions is, therefore, a feasible strategy to achieve complex curvature in 3D. Significant downsides are that the strategy is primarily applicable to soft elastic materials (such as gel sheets) and requires complicated programming of the shape-shifting or complex external stimuli to achieve the target shapes. Moreover, the in-plane distortions are likely to disturb any of the surface features that were imprinted on the 2D sheets, hence partially eliminating one of the major advantages that the 2D-to-3D shape-shifting offers. Fortunately, an alternative strategy that is more compatible with rigid materials and delicate surface features exists at the intersection of art and science: the use of *origami* (traditional Japanese paper folding) and *kirigami* (extended version of origami, also allowing cuts) to create, or at least approximate, complex curved shapes. Simply by imposing specific fold patterns, extended with cuts in the case of kirigami, initially flat sheets could be transformed into 2D or 3D geometries. Owing to their predictability, controllability, and scalability, origami and kirigami techniques have gained traction among scientists and engineers to develop deployable structures [25–27], reconfigurable metamaterials [28–32], self-folding robots [9,33], biomedical devices [34–37], and stretchable electronics [38–40]. Fig. 1 presents some examples of the potential applications of origami and kirigami across a range of length scales. By folding or cutting along the right patterns, origami and kirigami could transform planar sheets to approximate complex curved geometries, without the need for in-plane distortions.

In this review, the different origami and kirigami approaches to approximate surfaces with “double” (or “intrinsic”) curvature are discussed. We begin by providing a closer look at differential geometry and its links to origami, providing a more formal defi-

nition of the concepts “surface curvature” and “flat sheets”. Then, several origami techniques proposed to approximate curved surfaces are reviewed in the following section, followed by a section on recent advances in kirigami. We conclude by comparing the different techniques in terms of their suitability to approximate curved surfaces and discussing the practical aspects as well as providing an outlook on future directions and applications.

## Geometry of surfaces and origami

The notion of curvature could be somewhat ambiguous and may be applied to a range of geometrical objects, such as curves, surfaces, or higher dimensional manifolds (i.e. higher dimensional generalizations of surfaces). Here, we are interested in the curvature of surfaces, meaning how much the surface deviates from its tangent plane at a certain point. We briefly introduce the concepts that are crucial for understanding surface curvature in general and its relation to origami/kirigami.

### Defining surface curvature

It is useful to start the discussion of surface curvature by introducing the *principal curvatures*,  $\kappa_1$  and  $\kappa_2$ , at a given point on the surface. The principal curvatures are the maximum and minimum values of all the normal curvatures at that point (Fig. 2). The directions corresponding to these principal curvatures are the *principal directions* [41]. The principal curvatures and directions are a convenient way of indicating how the surface curves in the vicinity of a point on the surface. It is important to note that the principal curvatures cannot be uniquely determined at points where the normal curvatures are all equal. Such a point is called an *umbilical point*. The plane and the sphere are the only two surfaces that are entirely composed of umbilical points [41,42]. The principal curvatures can be combined to obtain two well-known measures of the curvature at a given point on the surface. The first measure is the *mean curvature*  $H$ , which is simply the mean of both principal curvatures:

$$H = \frac{1}{2}(\kappa_1 + \kappa_2)$$

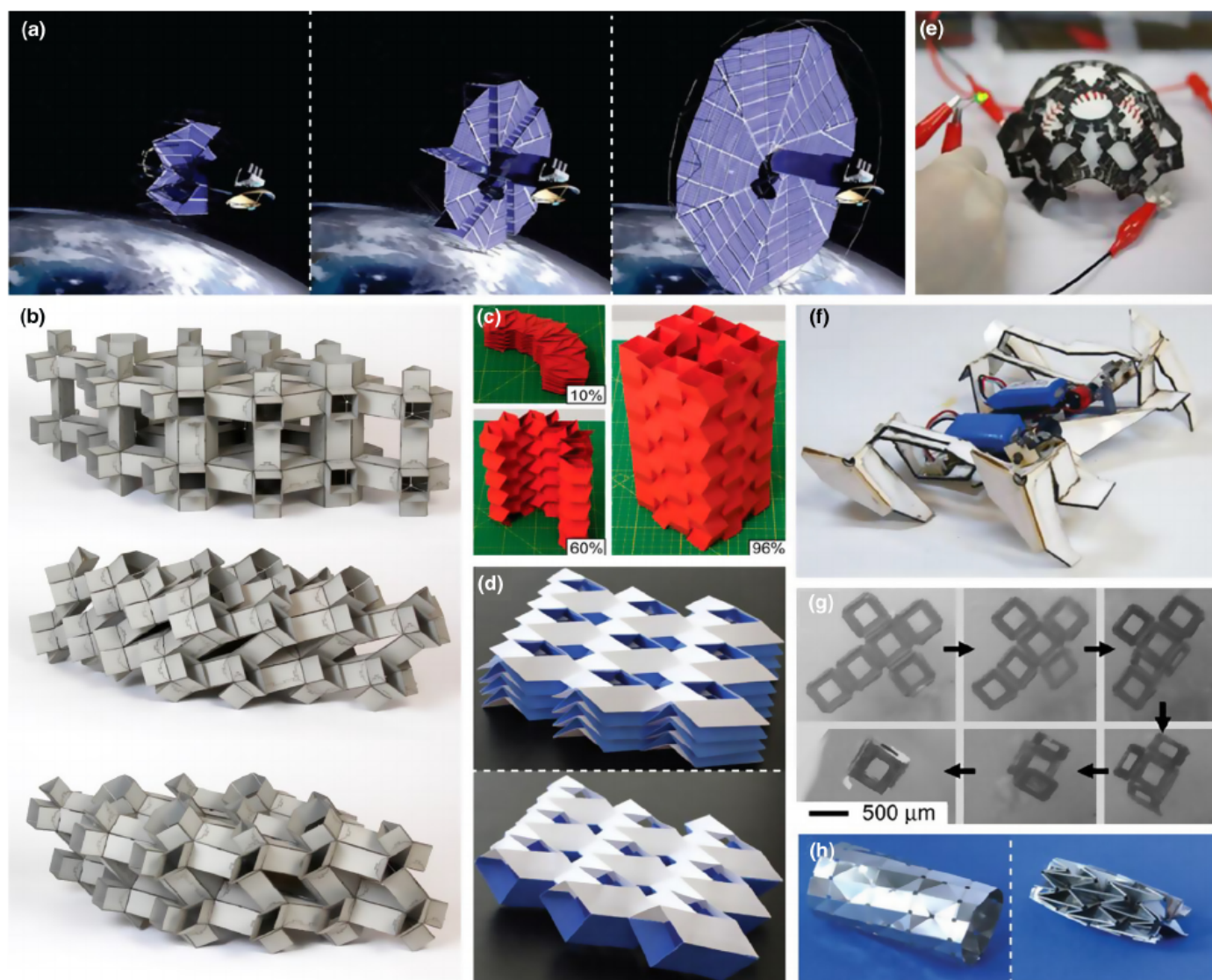
A flat plane has  $H=0$  since all normal curvatures are zero. However, when the plane is bent into a wavy shape (Fig. 2b), the mean curvature becomes non-zero at certain locations since one of the principal curvatures becomes non-zero.

The second useful measure of curvature is the *Gaussian curvature*  $K$ , defined as the product of the principal curvatures:

$$K = \kappa_1 \cdot \kappa_2$$

This concept was introduced in Gauss' landmark paper on *Theorema Egregium* (“remarkable theorem”), considered by some to be the most important theorem within differential geometry. It is clear from this definition that the Gaussian curvature at a certain point vanishes as soon as one of the principal curvatures is zero, in which case the point is called a “parabolic point”. When the principal curvatures are both non-zero and positive, the Gaussian curvature is positive and the point is termed “elliptic”. Finally, when the principal curvatures are non-zero and of opposite signs (i.e. the surface curves upwards in one direction and downwards in the other), the Gaussian curvature is negative, which corresponds to a “hyperbolic” point [41,42].



**FIGURE 1**

Various examples of scientific and engineering applications of origami and kirigami. (a) An artist's impression of an origami-based deployable solar array on space satellites (adapted with permission from ASME from Ref. [27]). (b) A cardboard prototype of a reconfigurable origami-based metamaterial (top), which has two degrees of freedom (middle and bottom). Adapted by permission from Macmillan Publishers Ltd: Nature [31], copyright 2017. (c) A deployable structure based on origami zipper tubes. Reproduced from Ref. [29]. (d) Paper versions of cellular metamaterials combining aspects from origami and kirigami. Reproduced from Fig. 3G and Fig. 3H of Ref. [32]. (e) A stretchable electrode based on a fractal kirigami cut-pattern, capable of wrapping around a spherical object while lighting an LED. Reproduced from Ref. [40]. (f) A centimeter-scale, crawling robot that is self-folded from shape-memory composites. Reproduced with permission from AAAS from Ref. [33]. (g) A biomedical application of origami: a self-folding microscale container that could be used for controlled drug delivery. Reproduced from Ref. [35] with permission from Elsevier. (h) Another biomedical application: a self-deployable origami stent based on the waterbomb pattern, developed by K. Kuribayashi et al. [34] (Reproduced with permission from Ref. [37]).

While both the mean and Gaussian curvatures could be defined in terms of the two principal curvatures, they represent a fundamentally different perspective on surface curvature. The mean curvature is an *extrinsic* measure of the surface curvature. This means that it depends on the way the surface is embedded in the surrounding three-dimensional space (which is Euclidean 3-space within the context of this paper). On the other hand, the Gaussian curvature is an *intrinsic* measure of the surface curvature, meaning that it is independent of the surrounding space and can be determined solely by measuring distances and angles within the surface itself [42–44]. In other words, the mean (extrinsic) curvature of the surface could only be determined by an observer outside of the surface that has knowledge of its surroundings, while the Gaussian (intrinsic) curvature of the sur-

face could be also determined by a 2D resident living on the surface that has no perception of the surrounding 3D space.

The distinction between these two types of curvature is important, as some surfaces might be extrinsically curved, but remain intrinsically flat. For example, it was already mentioned that bending of a flat plane into a wavy shape gives the surface a non-zero mean curvature. However, the Gaussian curvature of the surface is still zero since one of the principal curvatures is zero (Fig. 2b). Therefore, while the extrinsic curvature of a flat plane could be changed by bending it, its intrinsic curvature remains zero everywhere. Such a surface, having zero Gaussian curvature everywhere, is called a *developable surface*. In addition to the plane, three fundamental types of developable surfaces exist in 3D: the generalized cone, the generalized cylinder,





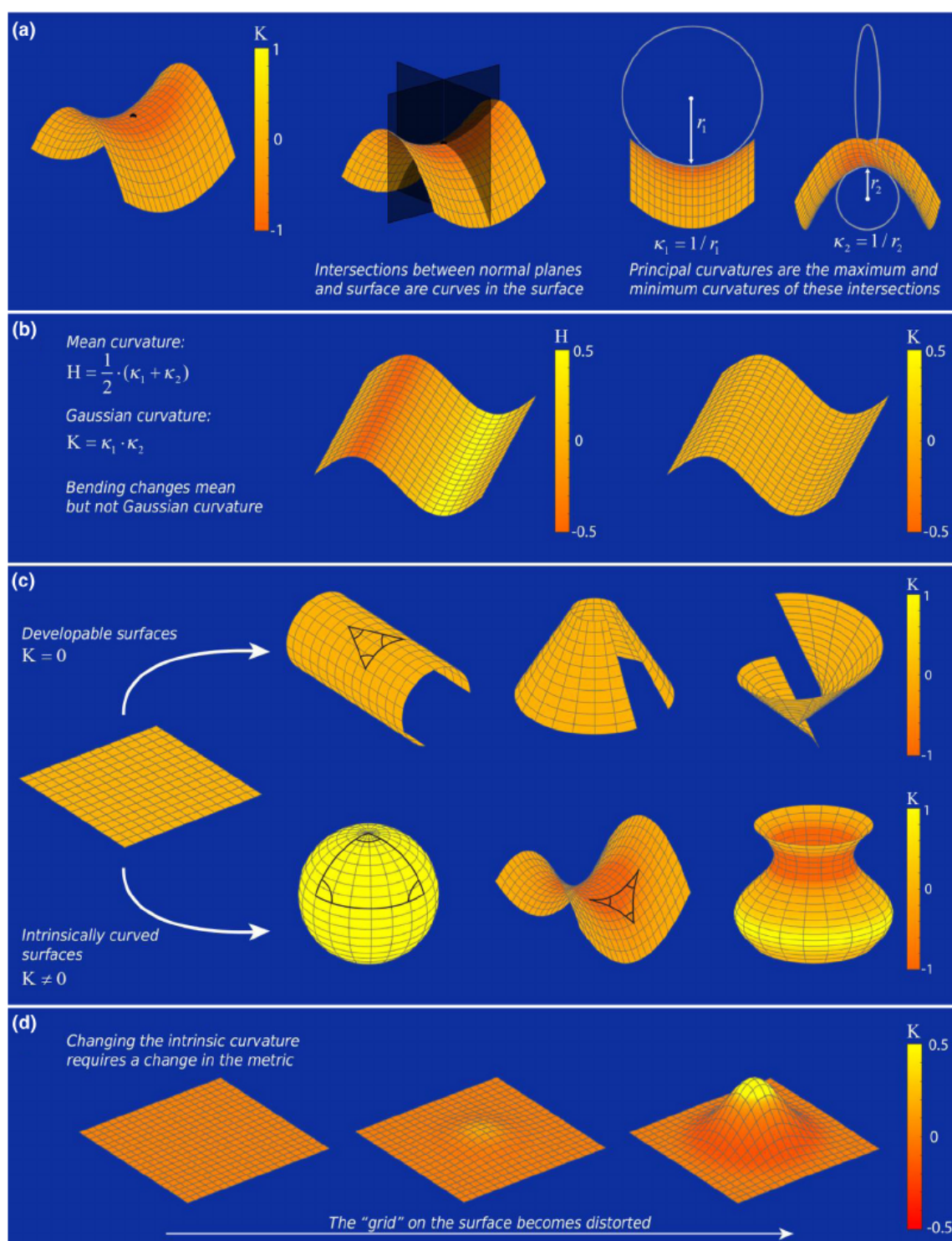


FIGURE 2

Measures of surface curvature. (a) The principal curvatures are calculated from the intersections between the normal planes at a point and the surface. The intersections form curved lines in the surface, with a certain "normal curvature". The maximum and minimum values of all possible normal curvatures are the principal curvatures, which are of opposite sign in this case given the fact that the surface curves "upward" in one direction and "downward" in the other. The color bar indicates the Gaussian curvature. (b) The mean and Gaussian curvatures could be calculated from the principal curvatures. Bending a planar surface could change the mean, or extrinsic, curvature (left figure, color bar indicates mean curvature), but not the Gaussian, or intrinsic, curvature (right figure, color bar indicates Gaussian curvature). (c) Transforming a planar surface (color bar indicates the Gaussian curvature). Top row: three types of developable surfaces which could be flattened onto the plane through bending. From left to right: a cylindrical surface, a conical surface, and the tangent developable surface of a space curve (a helix in this case). Bottom row: three types of intrinsically curved surfaces. From left to right: a sphere with  $K > 0$ , a saddle with  $K < 0$ , and a vase surface with varying  $K$ . The sum of the internal angles of a triangle drawn on an intrinsically curved surface does not equal  $\pi$ . (d) Interpreting relationship between the metric and the Gaussian curvature (color bar indicates Gaussian curvature). Creating the bell-shaped surface from an initially flat plane requires distortion of the grid on the plane.





the tangent developable to a space curve (Fig. 2c) [42,45,46]. The key feature of developable surfaces is that they could be constructed by bending a planar surface, without requiring extensional deformations. The observation that the Gaussian curvature of a flat plane does not change when bending the plane also holds more generally and forms the essence of Gauss' remarkable theorem: the Gaussian curvature is bending-invariant [42,47,48]. Arbitrary bending of any surface could therefore change its extrinsic (mean) curvature, but it cannot change the intrinsic (Gaussian) curvature of the surface. Consequently, a flat plane cannot be transformed into a spherical or saddle-shaped surface by bending deformations alone since these surfaces have non-zero intrinsic curvature (Fig. 2c).

We have stated that the Gaussian curvature is an intrinsic property of the surface, yet the classical definition that we have given above relies on extrinsic concepts, namely the principal curvatures. This is in fact the “remarkable” aspect in the Theorema Egregium of Gauss [42,47]. However, Gauss showed that the Gaussian curvature could also be defined on the basis of angle and distance measurements within the surface itself (i.e. intrinsically). A first understanding of this intrinsic description is obtained when considering a triangle drawn on the various surfaces, as shown in Fig. 2c. A triangle on the surface of the plane or any other developable surface ( $K = 0$ ) will always have the sum of its internal angles,  $\alpha_i$ , equal to  $\pi$ . However, on the surface of a sphere ( $K > 0$ ), the sum of the angles is larger than  $\pi$ , while on the surface of a saddle ( $K < 0$ ), the sum of the angles is smaller than  $\pi$  [43,47]. This angle measurement clearly relates to the intrinsic geometry of the surfaces, as a 2D resident of the surface that has no knowledge of the space in which the surface is situated could determine whether the surface has positive, negative, or zero Gaussian curvature, simply by measuring the angles of a triangle [43]. However, the resident would not be able to distinguish, for example, a flat plane from a cylinder surface since they both have the same (zero) intrinsic curvature.

A more formal “intrinsic” description of the Gaussian curvature requires the introduction of another important concept within differential geometry: the metric tensor, or simply *metric*. The metric of a surface describes the distances between the neighboring points on a surface which could be given as follows (in Einstein summation convention) [49]:

$$ds^2 = g_{ij} dx^i dx^j$$

where  $ds$  represents the distance between points and  $g_{ij}$  represents the metric components. In the case of a flat plane, the metric tensor (which is called a “Euclidean metric” in this case) is simply represented in Cartesian coordinates as:

$$g = \begin{pmatrix} 1 & 0 \\ 0 & 1 \end{pmatrix}$$

In which case  $ds^2$  reduces to the standard expression:

$$ds^2 = dx^2 + dy^2$$

Physically, the metric could be interpreted as a grid on the surface [50,51]. On a flat plane, this would be a regular grid consisting of equally spaced, perpendicular lines. When the flat plane is subjected to pure bending (see Fig. 2c), the grid is not distorted

and all distances and angles are preserved. For this reason, bending is called an *isometric* deformation, i.e. it leaves the metric unaffected. However, if the plane is deformed into, for example, a bell-shaped surface with regions of positive and negative Gaussian curvatures (Fig. 2d), the grid becomes distorted, i.e. the metric changes and becomes “non-Euclidean”. This simple interpretation of the metric as a grid on the surface, though not mathematically rigorous, does provide the important insight that we are aiming for: changing the Gaussian curvature requires a change in the surface metric (this leads to the inherent challenge that map-makers face: any map of the Earth will suffer some level of distortion [52]). Moreover, this change in metric (and thus in Gaussian curvature) cannot be achieved through bending alone but requires stretching or shrinking of the surface.

Gauss showed that the Gaussian curvature could be defined entirely in terms of the components of the metric tensor and its derivatives, thereby proving the intrinsic character of this curvature measure [47]. As a simple example, consider a 2D Euclidean metric defined in Cartesian coordinates of the form

$$g = \begin{pmatrix} 1 & 0 \\ 0 & \gamma(x) \end{pmatrix}$$

The function  $\gamma(x)$  describes the distances between points in the  $y$  direction as a function of  $x$ -position ( $ds^2 = dx^2 + \gamma(x)dy^2$ ). In this case, the Gaussian curvature is indeed defined entirely in terms of the metric as [47,49,50]:

$$K = -\frac{1}{\sqrt{\gamma}} \frac{\partial^2 \sqrt{\gamma}}{\partial x^2}$$

Following the above definition, the Euclidean, “flat” metric introduced earlier would indeed result in  $K = 0$ , or zero intrinsic curvature. The general definition of the Gaussian curvature in terms of the metric components and their derivatives will not be stated here, as this requires more advanced concepts from differential geometry which are outside the scope of this review. The reader interested in more detailed mathematical accounts of Gauss' results is referred to several excellent sources [47,48,52].

The direct relation between the surface metric and Gaussian curvature has been harnessed by several researchers to controllably transform flat sheets into intrinsically curved geometries [19–21,53,54]. As explained by Klein et al., this could be achieved by prescribing a non-Euclidean “target metric” in the flat sheet which essentially means that a non-uniform expansion or contraction distribution is “programmed” into the sheets [19]. Upon activation by an external stimulus, differential swelling/shrinking occurs, which is accommodated by deforming into a curved 3D geometry in accordance with the newly imposed metric. Hence, these “metric-driven” [20] approaches represent a successful application of Gauss' results to the shape-shifting of advanced materials. However, an important remark is that these approaches deal with real sheet materials of a small but finite thickness, while our discussion thus far has only considered mathematical surfaces of zero thickness. The presence of thickness forces researchers to consider the elastic energy of curved sheets, consisting of a stretching component ( $E_s$ ) and a bending component ( $E_b$ ), both of which depend on the sheet thickness [19,53,55]:



$$E = E_s + E_b$$

When a non-Euclidean target metric is prescribed in the flat sheet with finite thickness, the sheet will adopt a shape that minimizes its elastic energy  $E$ . This leads to a competition between both components of the energy: the bending energy  $E_b$  is zero when the sheet remains flat, while the stretching energy  $E_s$  is zero when the sheet achieves the curved, 3D geometry with the prescribed target metric [19,49,53]. The final shape corresponds to a balance between both contributions, which is determined by the sheet thickness  $t$ . Since the stretching energy scales with  $t$  and the bending energy scales with  $t^3$ , there will be a certain thickness that marks a transition between bending energy domination and stretching energy domination [49,56]. Consequently, the thinner a sheet becomes, the more energetically favorable it becomes to bend than to stretch [49,51,53]. In other words, the bending energy decreases more rapidly with decreasing thickness than the stretching energy does, meaning that when given the choice between bending or stretching to accommodate local shrinking/swelling, it will “cost” much more energy for the thin sheets to stretch than to bend (which is why very thin sheets are often considered inextensible membranes [55]). The sheets will thus bend in 3D to adopt the target metric (if a suitable embedding of the target metric exists), although the exact target metric will not be achieved for finite thickness since there will always be some energetic cost to bending a sheet [19,53].

In summary, the concept of surface curvature could be discussed from an extrinsic and an intrinsic perspective, using the mean and Gaussian curvature respectively. Some surfaces might be curved from an extrinsic view, yet intrinsically remain flat (a developable surface). When the aim is to achieve extrinsic curvature from a flat surface, this could be easily achieved by an inextensional bending (isometric) deformation of the surface, which leaves the Gaussian curvature unaffected. However, achieving intrinsic (Gaussian) curvature from a flat surface is more complicated, as it requires the distances between points on the surface to change (i.e. the metric should change). This cannot be achieved through bending alone, but requires in-plane stretching or shrinking of the surface. The geometrical aspects of origami introduced in the following section are better understood within the context of the ideas presented here.

### Geometrical aspects of origami

Origami has inspired artists for hundreds of years to transform ordinary sheets of paper into intricate yet beautiful 2D or 3D geometries. Recently, engineers and scientists have also become attracted to origami and have studied the paper-folding art from a more mathematical perspective, giving rise to the field of *computational origami* [57]. Origami offers many interesting mathematical challenges, such as the folding of an arbitrary polyhedron from a flat piece of paper [58] or the question of flat foldability, i.e. whether a crease pattern results in a folded state having all points lying in a plane [59]. Another aspect that has received broad attention and that is of greater relevance to the folding of 3D engineering structures is the question of *rigid-foldability*. An origami design is rigid-foldable if the transition from the flat to the folded state occurs smoothly through bend-

ing at the creases only, thus, without bending or stretching the faces in between the creases. In other words, a rigid origami design could be folded from rigid panels connected with hinges, which is desirable for deployable origami structures made from rigid materials, such as solar panels, medical stents, or robots [60,61].

Classical origami starts with a flat sheet of paper, which could be considered a developable surface and by definition has zero Gaussian curvature. Folding this flat sheet along predefined crease lines essentially means bending the sheet at a very high radius of curvature. Since bending does not change the metric of the sheet, the Gaussian curvature will remain zero at (near) all points on the folded sheet. In other words, no matter how the sheet is folded, it remains intrinsically flat. It must, however, be noted that some degree of stretching is involved in the folding of paper. More specifically, Witten [55] has explained that sharp folds must involve some stretching, as they would otherwise result in an infinitely high bending energy. Nevertheless, the stretching is only confined to the small fold lines and it is typically neglected, i.e. a non-stretchable sheet with idealized sharp folds is assumed [62].

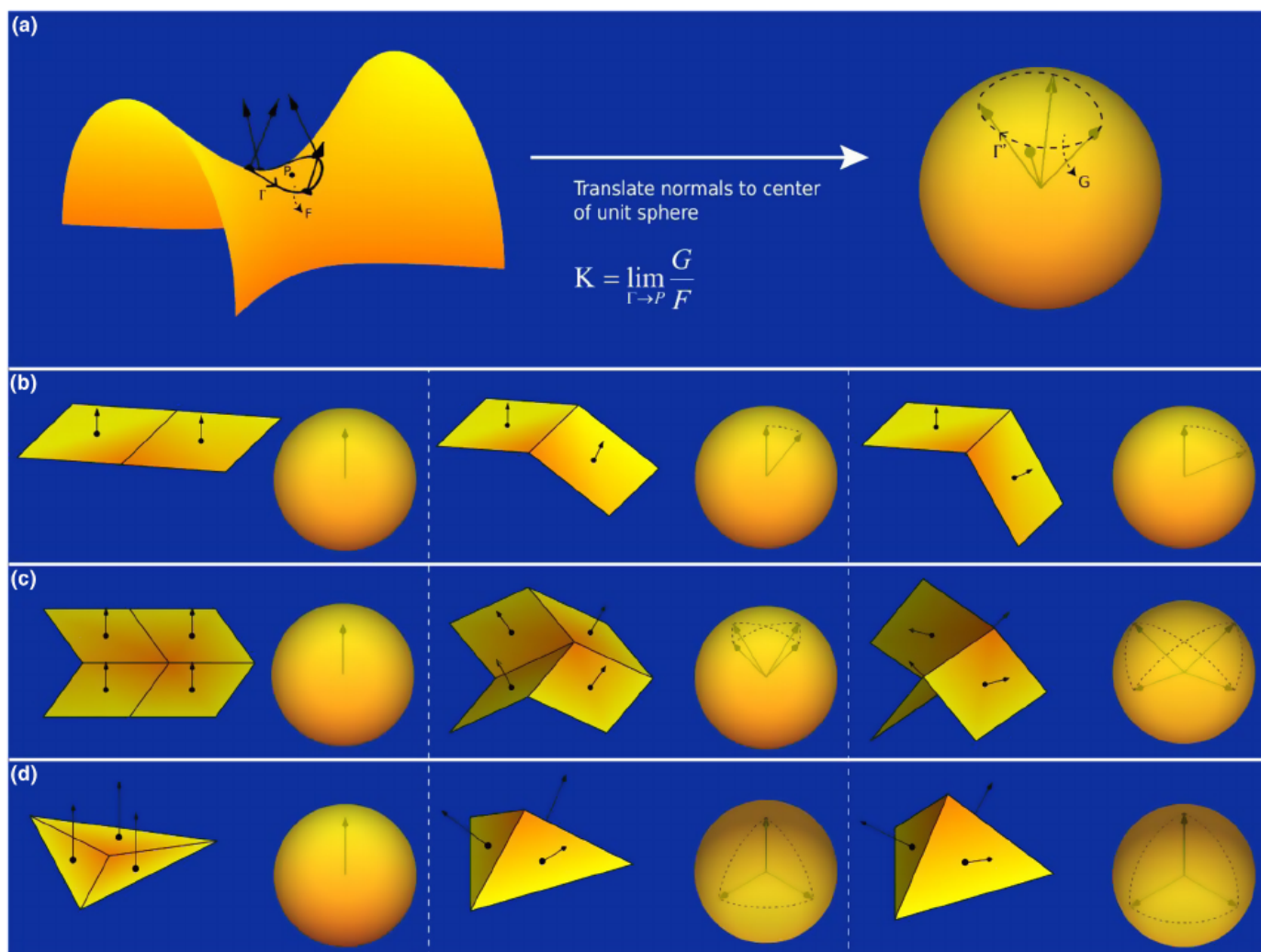
When discussing origami and polyhedral surfaces, it is useful to introduce yet another definition of the Gaussian curvature, known as Gauss' spherical representation. Gauss introduced this description in his original paper on the *Theorema Egregium*. This concept has been used, for example, by Miura [63] and Huffman [64] in the analysis of origami. Gauss' spherical representation could be obtained by first considering a closed, oriented contour  $\Gamma$  around a point  $P$  on an arbitrary surface (Fig. 3a). Let us collect the unit vectors on  $\Gamma$  that are normal to the surface and translate them to the center of a unit sphere (the Gauss sphere), effectively tracing out a new oriented contour  $\Gamma'$  on the surface of the sphere and obtaining the “Gauss map” of the original contour. Both contours enclose a certain area on their respective surfaces: say  $\Gamma$  encloses  $F$  and  $\Gamma'$  encloses  $G$ . The Gaussian curvature  $K$  is then defined as the ratio of  $G$  to  $F$ , in the limit that  $\Gamma$  approaches  $P$  [42,65]:

$$K = \lim_{\Gamma \rightarrow P} \frac{G}{F}$$

While calculating the Gaussian curvature on an arbitrary surface might not be trivial using the above definition, Gauss' spherical representation does provide an additional interpretation of the intrinsic curvature. For example, the Gauss map of a closed contour on a developable surface encloses zero area on the Gauss sphere ( $G = 0$ ), indeed corresponding to zero Gaussian curvature following the above definition (Fig. 3). On the other hand, closed contours on spherical or saddle surfaces map into closed contours with non-zero enclosed areas on the Gauss sphere, indicating the non-zero Gaussian curvature of these surfaces. Note that  $G < 0$  when the orientation of  $\Gamma'$  is opposite to that of  $\Gamma$ , resulting in a negative Gaussian curvature (Fig. 3a) [65].

Applying Gauss' spherical representation to the simplest type of origami, a single straight crease crossing a flat sheet of paper, once again proves that folding has no intrinsic effect on the surface. The normals on each face map into a single point on the Gauss sphere, while the normals on the crease between the faces are uniquely defined and map into an arc connecting both points.



**FIGURE 3**

Gauss' spherical representation of the Gaussian curvature. (a) Definition of the Gauss map using a closed, oriented contour on a point on an intrinsic curved surface. The unit normals on  $\Gamma$  are translated to the center of a unit sphere and trace out a new contour  $\Gamma'$ . (b) Folding along a simple straight crease does not change the Gaussian curvature (note the zero enclosed area on the unit sphere). In the flat state (left pane), all the normals point in the same direction, resulting in no enclosed area on the unit sphere. In the folded configuration, both are connected on the unit sphere through a zero-area arc. (c) Gauss map applied to a unit cell of the rigid-foldable Miura-ori pattern. In the partially folded configurations (middle and right pane), the normals trace out a bowtie contour on the Gauss sphere, with one-half of the bowtie classifying as "positive" area (clockwise tracing) and the other half as "negative" area (counter-clockwise trace), resulting in zero net area. (d) The Gauss map applied to the three-valent vertex of a tetrahedron. The transformation of the flat state (left pane) to the folded state (middle and right pane) induces a change in the Gaussian curvature (non-zero area on the unit sphere), showing that a three-valent vertex cannot be achieved in rigid origami.

resulting in  $G = 0$  and, thus, no Gaussian curvature (Fig. 3b) [44]. Miura [63] used Gauss' spherical representation to analyze different configurations of fold lines joining at a common vertex and showed that some combinations cannot be folded rigidly [63]. For example, a vertex of valency three (three creases joining at the vertex) is never rigid-foldable: the three faces surrounding the vertex have normals in different directions, tracing out a spherical triangle on the Gauss sphere with non-zero area (Fig. 3d). This would imply that  $K \neq 0$ , which is not possible when rigidly folding a flat surface. Similarly, Miura showed that a four-valent vertex with all mountain ("upwards") or valley ("downwards") folds cannot be folded rigidly, while a four-valent vertex with three mountain folds and one valley fold (and vice versa) could be rigidly folded [63,65]. It must be, however, emphasized that a three-valent vertex or a four-valent vertex with all mountain folds could be folded when the rigid folding requirement is relaxed, i.e. when the faces are allowed to bend.

Based on the above insights, it might be argued that origami is not a suitable approach to create intrinsic curvature from flat sheets as origami deals with isometric deformations. However, applying the right fold and cut patterns could alter the "intrinsic" or "apparent" Gaussian curvature, without the need for in-plane stretching or shrinking of the flat sheet. In essence, origami and kirigami techniques allow to *approximate* intrinsically curved surfaces through developable deformation of many small faces connected through fold lines. The specific origami and kirigami techniques that have been used by other researchers for this purpose are described in the next section of this review. Note that we will restrict to the traditional form of origami in which flat (Euclidean) sheets are folded. It is, however, also possible to apply origami to non-Euclidean paper, as shown by Alperin et al. [66] who folded an origami crane from hyperbolic paper, i.e. paper with constant negative curvature.





## Origami approaches

In this section, we will review different origami approaches that have been used to approximate intrinsically curved surfaces. The four different approaches discussed here, namely origami tessellations, tucking molecules, curved-crease origami, and concentric pleating, all start from a flat, uncut sheet that is folded along predefined creases.

### Origami tessellations

Origami tessellations, characterized by a periodic crease pattern or “tiling” of a flat sheet, have inspired artists for many decades [67] but have also found their way into scientific and engineering applications such as compliant shell mechanisms [68] and mechanical metamaterials [30,69]. Moreover, the rational design of the tessellation pattern allows for changing the apparent curvature of flat sheets without requiring local stretching of the faces.

#### Miura-ori

The most widely studied origami tessellation is the herringbone pattern known as *Miura-ori*, originally introduced as an efficient

packing of solar sails [25] but also observed in spontaneous wrinkling of thin, stiff films on thick, soft substrates subjected to biaxial compression [70]. A Miura-ori unit cell consists of a four-valent vertex connecting four parallelograms using three mountain folds and one valley fold (Fig. 4). An important property of this origami design is that it is rigid-foldable, as indicated by Gauss’ spherical representation [63,65] (Fig. 3c). Schenk and Guest studied the geometry and kinematics of Miura-ori and showed that purely rigid Miura-ori has only a single degree of freedom, i.e. in-plane folding and unfolding [28]. Based on a detailed analysis of a single unit cell, they concluded that a Miura-ori sheet is an auxetic material, characterized by a negative in-plane Poisson’s ratio. In a later study, however, Lv et al. showed that some specific configurations could exhibit a positive in-plane Poisson’s ratio as well [71]. While rigid-foldability of Miura-ori allows only in-plane deformations, experiments with simple paper models reveal that the folded sheets could also deform out-of-plane (Fig. 4d-e). Indeed, Schenk and Guest identified saddle and twist deformation modes and showed that these are only possible in non-rigid Miura-ori, where the individual faces are allowed to bend [28]. This leads to an interesting

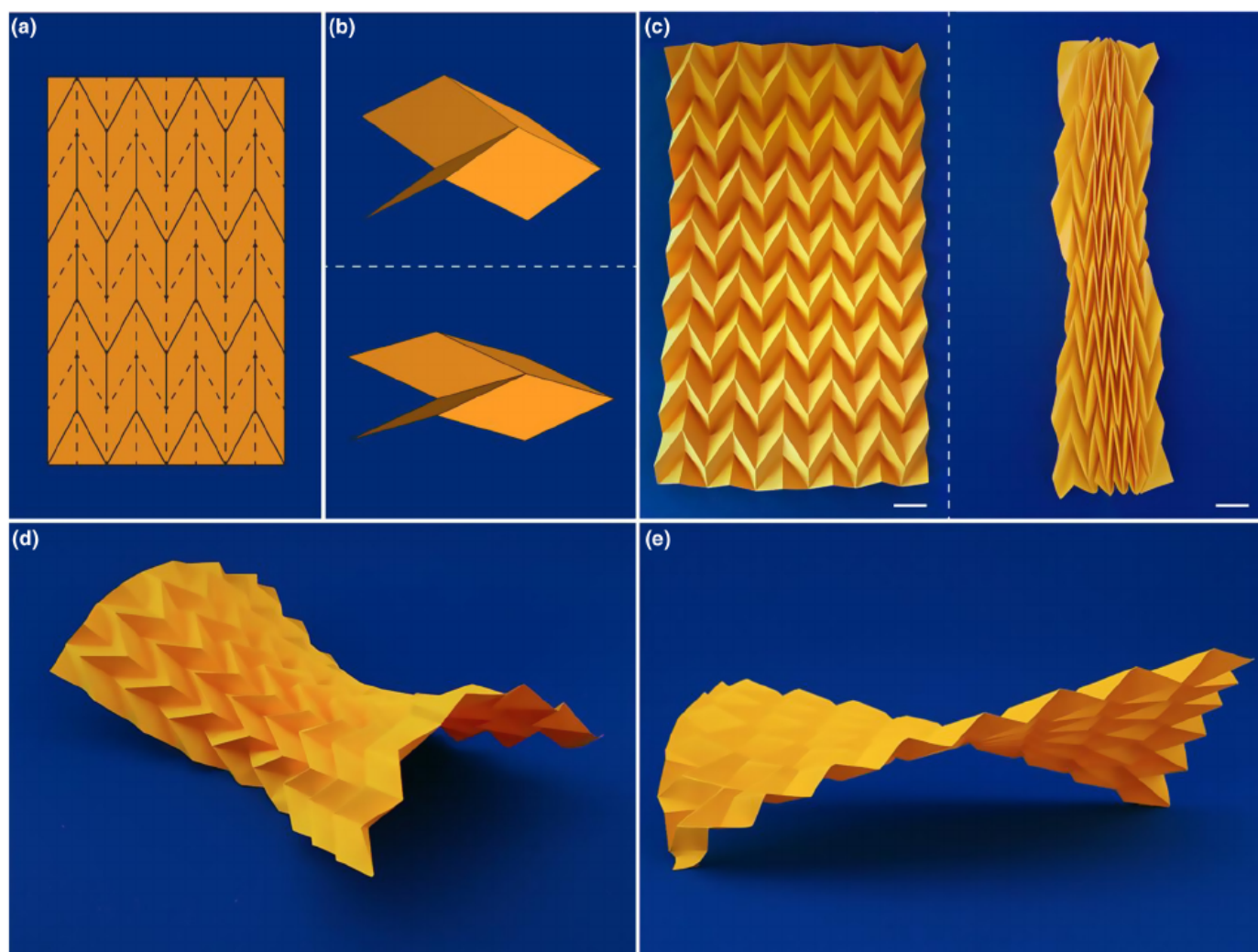


**FIGURE 4**

Miura-ori tessellation. (a) A crease pattern of a Miura-ori tessellation. Solid lines are mountain folds and dashed lines are valley folds. (b) Two different unit cells for a Miura-ori tessellation, consisting of four parallelograms connected through three mountain folds and one valley fold. (c) A paper model of Miura-ori tessellation in a partially folded state (left) and collapsed state (right), showing the flat-foldability of this origami pattern (Scale bar is 2 cm). Saddle-shaped and (e) twisted out-of-plane deformations of the (non-rigid) Miura-ori sheet.





property of Miura-ori (and origami tessellations in general): through developable deformations at unit cell level, the *global* Gaussian curvature of the sheet could be changed, making this origami tessellation an interesting candidate for compliant shell mechanisms [68,72].

Several researchers have sought for generalizations or variations of the Miura-ori pattern that approximate a curved surface when folded, without requiring out-of-plane deformations. Tachi investigated quadrilateral mesh origami consisting of quadrilateral faces joined at four-valent vertices and established rules for rigid-foldability. Starting from a regular Miura-ori pattern, he explored variations that could fit a freeform surface (e.g. a dome-shape), while remaining rigidly foldable [73]. Gattas et al. parameterized the Miura-ori to be able to systematically compare different pattern variations. They investigated five rigidly foldable “first-level derivatives” obtained by changing a single characteristic such as the crease orientation [74]. Depending on the derivative, geometries with an overall single or double curvature could be achieved, although the latter seemed to be limited to a non-developable crease pattern [74]. Sareh and Guest considered Miura-ori as one of the seventeen plane crystallographic or “wallpaper” groups (a *pmg* group) and provided a framework to obtain flat foldable symmetric generalizations of the Miura-ori, some of which could result in globally curved geometries when folded [75]. More recently, Wang et al. proposed a design method to obtain Miura-ori generalizations that approximate cylindrical surfaces upon folding [76]. While their method takes into account rigid folding and the thickness of the faces, which is useful for practical applications, it is restricted to cylindrical geometries and hence single curvature [76]. Per-

haps the most complete and successful approach to approximating arbitrarily curved surfaces with Miura-ori generalizations is one recently proposed by Dudte et al. (Fig. 5) [77]. Dudte et al. employed constrained optimization algorithms to solve the inverse problem of fitting an intrinsically curved surface with a generalized Miura-ori tessellation. They showed that the surface of generalized cylinders could be approximated using flat foldable and rigid-foldable tessellations, which could not be guaranteed for intrinsically curved surfaces. In the latter case, snapping transitions were required during the action of folding or unfolding, although the final configuration was strain-free [77]. The researchers also showed that a higher number of unit cells resulted in a more accurate fitting of the surface but at the cost of a higher folding effort [77].

#### Other periodic tessellations

In addition to Miura-ori, several other tessellations are known among origami artists and scientists. Examples are other tessellations obtained when tiling the plane with a six-fold or eight-crease waterbomb base, the former of which has been used to create an origami stent [34,78]. Other famous origami tessellations were developed by Ron Resch [79,80] and have inspired scientists to create origami-based mechanical metamaterials [79]. Freeform surface approximations [81]. Origami tessellations that are rigid-foldable are of particular interest for engineering applications. Evans et al. used the method of fold angle multiplication to analyze the existing flat foldable tessellations and identified those that were rigid-foldable [61]. Furthermore, the researchers presented rigid-foldable origami “gadgets”, local modifications to a crease pattern, to develop new rigidly foldable tessellations.

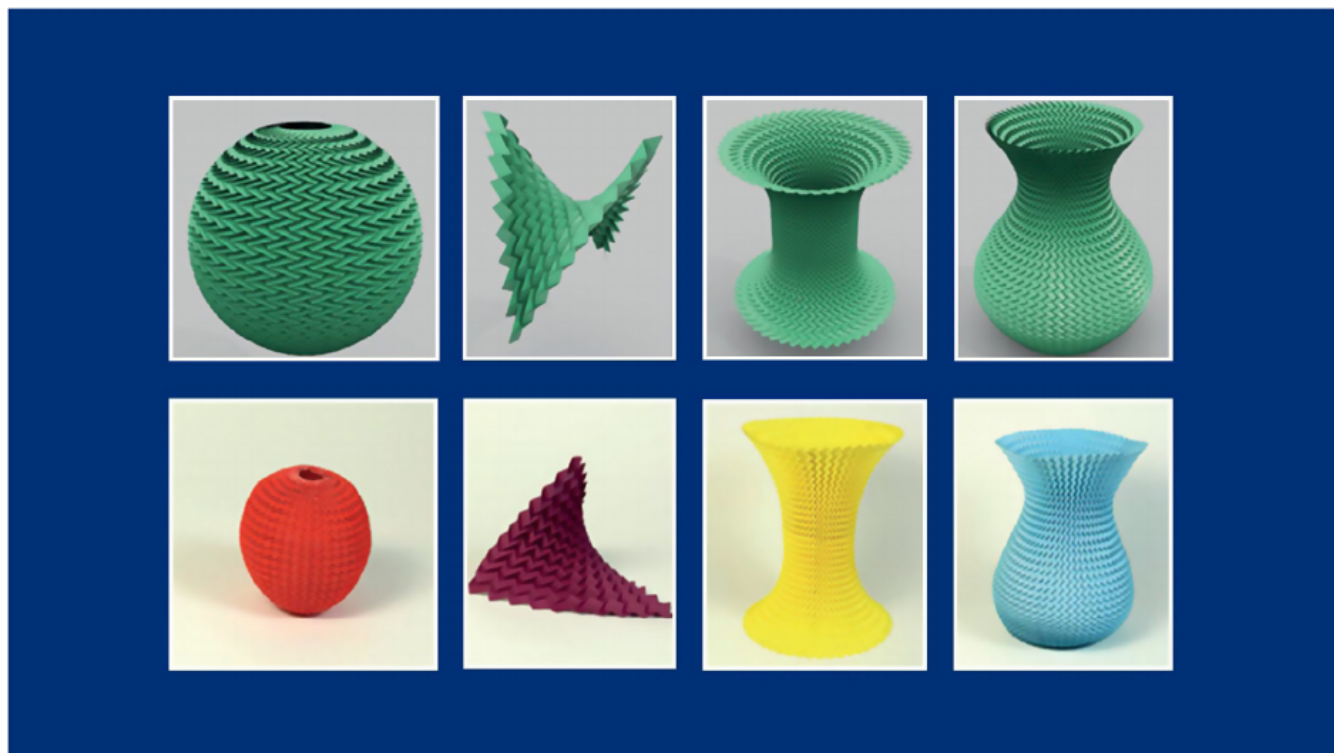


**FIGURE 5**

Generalized Miura-ori tessellations fitting curved surfaces. The top row depicts simulations, while the bottom row shows physical models. Adapted with permission from Macmillan Publishers Ltd: Nature Materials [77] copyright 2016.



[61]. Tachi studied the rigid foldability of “triangulated” origami tessellations, in which the quadrangular faces are divided into triangles (essentially capturing the bending of faces of non-triangulated origami) [82]. Through numerical simulations (by means of a truss model), it was observed that most periodic triangulated origami tessellations exhibit two (rigid) degrees of freedom, a folding/unfolding motion and a twisting motion, with Miura-ori being an exception as it only shows the folding/unfolding motion [82].

Applying a periodic tessellation such as Resch’s triangular pattern to a flat sheet essentially means texturing the sheet with small-scale structures that give rise to unusual properties on a global scale [72]. Due to the strong interaction between the local kinematics and global shape, these tessellated sheets have earned the name “*meta-surfaces*”, in analogy with 3D metamaterials [68,72]. An interesting property of the textured sheets is that folds may partially open or close locally, effectively simulating local stretching or shrinking. As a consequence, the sheets could undergo large deformations and change their global Gaussian curvature, without stretching of the actual sheet material [68,72] (Fig. 6). However, the opportu-

nities to approximate curved surfaces using this approach are limited despite the ease with which small paper models can be manipulated. That is because approximating saddle shapes might involve some facet and crease bending that makes it difficult, if not impossible, to achieve anticlastic geometries (negative Gaussian curvature) through rigid folding [81]. Moreover, for large tessellated sheets (with many unit cells), even synclastic geometries (positive Gaussian curvature) might not be rigid-foldable. Tachi showed that smooth rigid folding of (triangulated) periodic tessellations in dome shapes is obstructed once the tessellated sheet becomes too large, making only cylindrical surfaces feasible [82]. A similar conclusion was reached by Nassar et al. [83]. Indeed, the tessellation shown in Fig. 6c naturally adopts a cylindrical shape in the partially folded configuration.

Although several standard origami tessellated sheets can conform to curved surfaces, the achievable geometries are limited. In order to obtain more complex 3D shapes, Tachi developed the *Freeform Origami* method to generalize existing tessellations, essentially building further on his work on quadrilateral mesh origami [84]. He provided mathematical

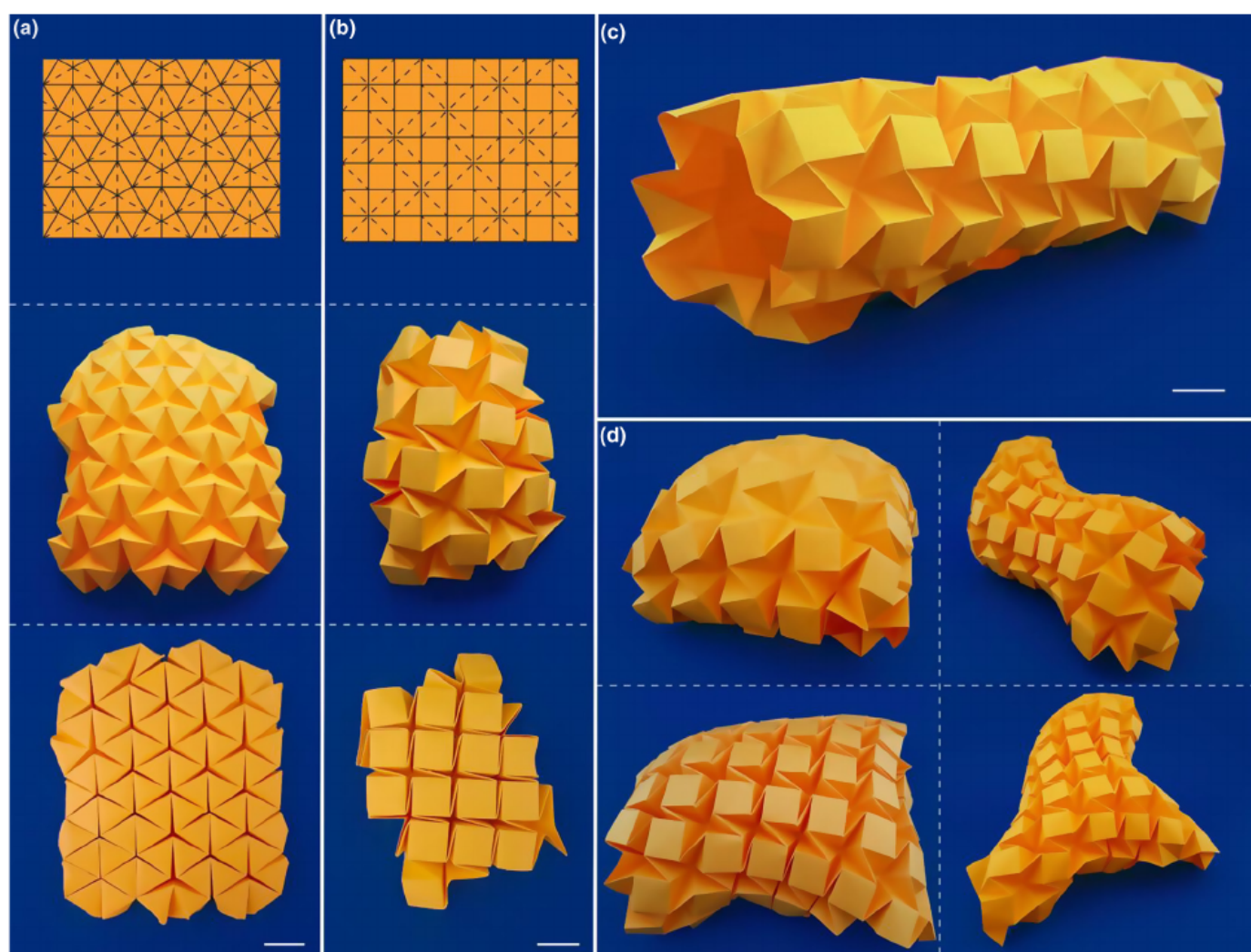


**FIGURE 6**

Origami tessellations. (a and b) Triangular Ron Resch and square waterbomb tessellations, respectively. Top: crease pattern (solid lines are mountain folds, dashed lines are valley folds), middle: partially folded state, bottom: fully folded state (Scale bar is 2 cm). (c) Natural resting state of the partially folded square waterbomb tessellation (for a large enough sheet), adopting a cylindrical shape (Scale bar is 2 cm). (d) Various configurations with global intrinsic curvature obtained from the same square waterbomb tessellated sheet, obtained through locally opening and closing the unit cells.





descriptions of the conditions that apply to the traditional tessellations such as developability and flat-foldability, and numerically calculated perturbations of these tessellations while preserving those conditions. The algorithm was implemented in a software package that allows the user to actively disturb an existing folded origami tessellation and observe the corresponding changes to the crease pattern in real-time [84]. However, the software is not capable of solving the inverse problem of finding the crease pattern that belongs to a given 3D surface. Other researchers have also used mathematical methods to calculate new tessellations that could fold into 3D geometries. Zhou et al. proposed the “vertex method” to inversely calculate a developable crease pattern based on the Cartesian coordinates of a given 3D geometry [85]. While their method is versatile enough to develop the crease pattern for a structure that fits between two (single-) curved surfaces, a major limitation is that it is not applicable to intrinsically curved surfaces [85]. More recently, Song et al. built further on this work and developed a mathematical framework to create trapezoidal crease patterns that rigidly fold into axisymmetric double-curved geometries [86]. More specifically, their method calculates the crease pattern that fits both an inner and outer target surface with the same symmetry axis. While intrinsic curvatures could in this way be achieved, the proposed method is limited to very specific ring-like geometries, possessing rotational symmetry and having relatively small curvatures [86].

### Tucking molecules

Other approaches to approximate intrinsically curved surfaces could be obtained from the field of computational *origami design*, in which one searches for the crease pattern that belongs to a given shape, typically a 3D polyhedron. The first well-known computational tool facilitating origami design was proposed by Lang and is based on tree-like representations of the desired shapes (“stick-figures”) [87]. However, the method is restricted to calculating origami bases that need to be shaped afterward into the desired geometry. To enable the construction of crease patterns for arbitrary 3D polyhedrons, Tachi developed his well-known “origamizing” approach based on *tucking molecules* [59,88]. The starting point is a polyhedral representation of an arbitrary surface, which is made topologically equivalent to a disk (such that it is not a closed polyhedron but has a cut that allows it to open). The basic idea of the approach is to map all the surface polygons of the polyhedron onto a plane and to fill the gaps in between with tucking molecules, which are flat foldable segments, creating a 2D crease pattern in doing so [88]. The resulting crease pattern is not considered an origami tessellation in the context of this review as it is highly non-periodic and comprises polygons of different shapes and sizes. The tucking molecules connect adjacent surface polygons and are tucked away behind the visible surface upon folding (Fig. 7a). Tachi defined edge-tucking and vertex-tucking molecules, respectively bringing edges or vertices together in the folded configuration. In order to fit the desired 3D shape with the surface polygons, crimp folds are also employed to locally adjust the tucking angle [88]. The entire procedure was implemented in a software package for which the input is a polygon mesh and the output is a 2D crease pattern, allowing the creation of complex origami structures that

were never folded before, such as the origami Stanford bunny (Fig. 7c) [59]. Tachi attributed the increased practicality of this approach compared to earlier origami design methods to three reasons: multi-layer folds rarely occur, the crimp folds offer structural stiffness by keeping vertices closed, and the method has a relatively high efficiency, defined by the ratio of polyhedral surface area to required paper area [59]. Despite its versatility and generality, the origamizing method has the drawback that some 3D polyhedrons cannot be mapped into a 2D pattern, a problem that was recently addressed by Demaine and Tachi [89], or that the proposed pattern is inefficient. Moreover, the flat foldability requirement of the tucking molecules significantly reduces the applicability of this method to the folding of stiff, thicker materials [81]; and the presence of crimp folds obstructs smooth folding [59], making this method intractable for industrial applications.

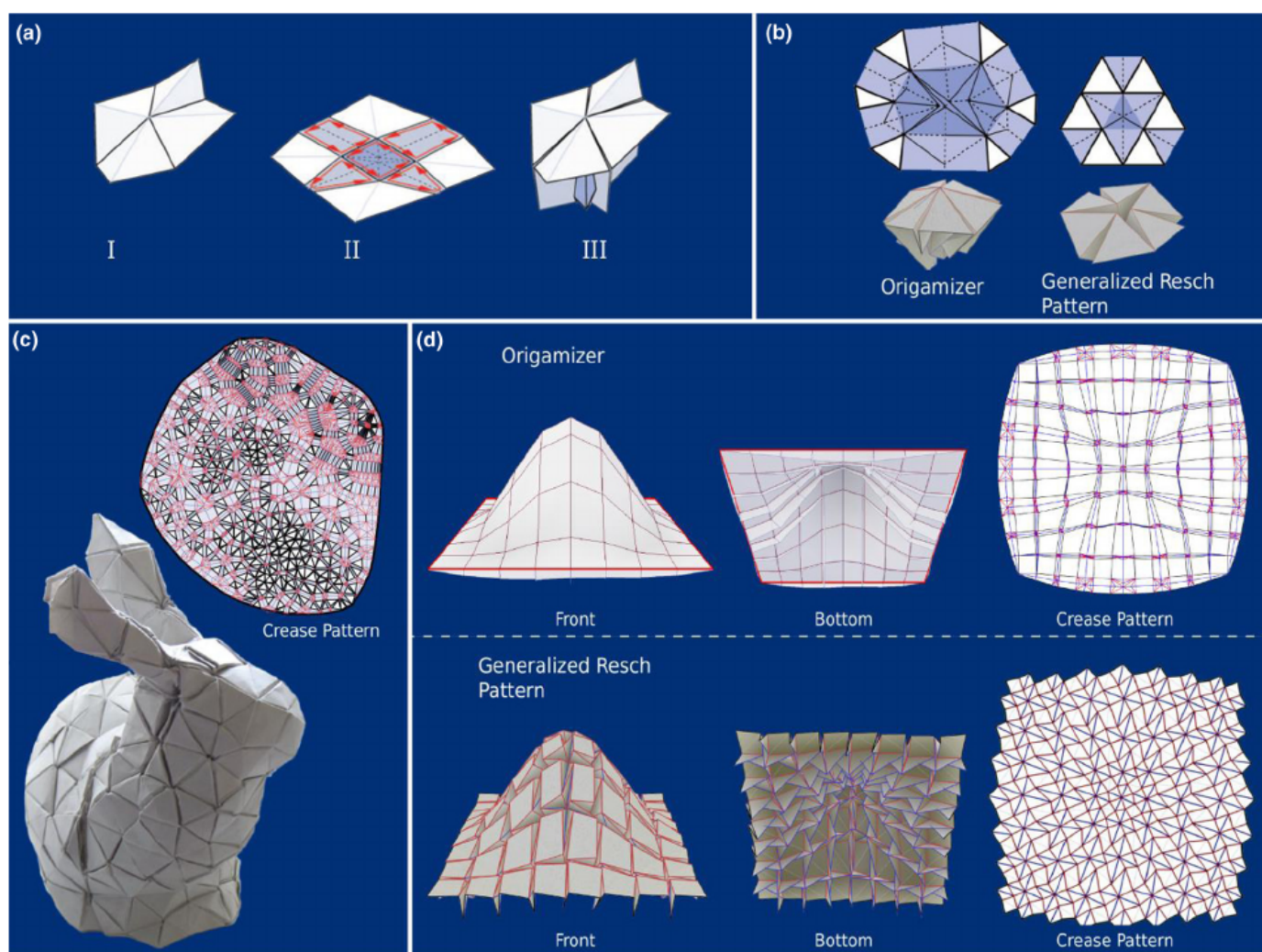
Tachi also proposed a more practically applicable method to approximate curved surfaces, combining aspects from his earlier work on freeform origami [84] and the origamizing approach [88]. The basic idea is that generalizations of Resch’s tessellations are calculated that fit a given polyhedral surface [81]. Contrary to the origamizing approach, the surface polygons do not have to be mapped onto the plane; but a first approximation of the tessellation is directly obtained from the 3D structure, after which it is numerically optimized to become developable and to avoid collisions of faces. As such, the implementation of this method is related to the earlier work on *Freeform Origami* [84], but it is not considered in this section since (simple) tucking molecules are used. Tachi defined a “star tuck” and variations thereof as building blocks to tessellate the given 3D surface [81]. The fundamental difference between conventional tucks and the star tuck is that the latter could also exist in a semi-folded state and do not have to be folded flat (Fig. 7b). The surface polygons could be arranged to locally fit the desired shape through partial opening of the star tucks, while this required crimp folds in the origamizing approach. The algorithm was implemented in a software package, allowing users to interactively design the generalizations of Resch tessellations corresponding to a given surface (Fig. 7c). However, for highly complex surfaces, which would require significant stretching and shrinking to become developable, crease patterns cannot always be generated. Moreover, smooth folding of the tessellations is not guaranteed for all cases. Nonetheless, the proposed method has significant potential for the practical folding of advanced materials into intrinsically curved surfaces.

### Curved-crease origami

When discussing curvature and origami, it is natural to also consider curved-crease origami. While this variant of traditional origami has interested artists for several decades, the mathematical study of curved-crease folding is underexplored and practical applications of origami have been primarily limited to straight creases [90]. Straight-crease and curved-crease origami is fundamentally different since both faces adjacent to a curved crease *always* have to bend in order to accommodate the folding motion [91,92]. In other words, curved-crease origami is never rigid-foldable. As a consequence, curved-crease origami cannot be reduced to a matter of tracking vertex coordinates as in the case of rigid origami.





**FIGURE 7**

Origami involving tucking molecules. (a) The definition of a tucking molecule used in the “Origamizer” approach. (I) A section of a polyhedral surface, (II) flattened polyhedral surface, showing the surface polygons connected through edge- and vertex-tucking molecules. (III) The folded configuration, showing the excess material being tucked away behind the outer surface. Reproduced with permission from IEEE from Ref. [59]. (b) Comparison between tucking molecules in the “Origamizer” approach and the generalized Ron Resch tessellation approach. Reproduced with permission from ASME from Ref. [81]. (c) Origami Stanford bunny, folded from a single-sheet crease pattern created using the “Origamizer” software. Reproduced from Fig. 1 from Ref. [89]. (d) Comparison between the surface approximations of the “Origamizer” approach (top) and the generalized Ron Resch pattern approach (bottom) to an intrinsically curved bell-shaped surface. Note the partially opened tucking molecules in the latter approach. Figures and crease patterns were obtained using “Origamizer” [59] and “Freeform Origami” [73] (red lines are mountain folds, blue lines are valley folds).

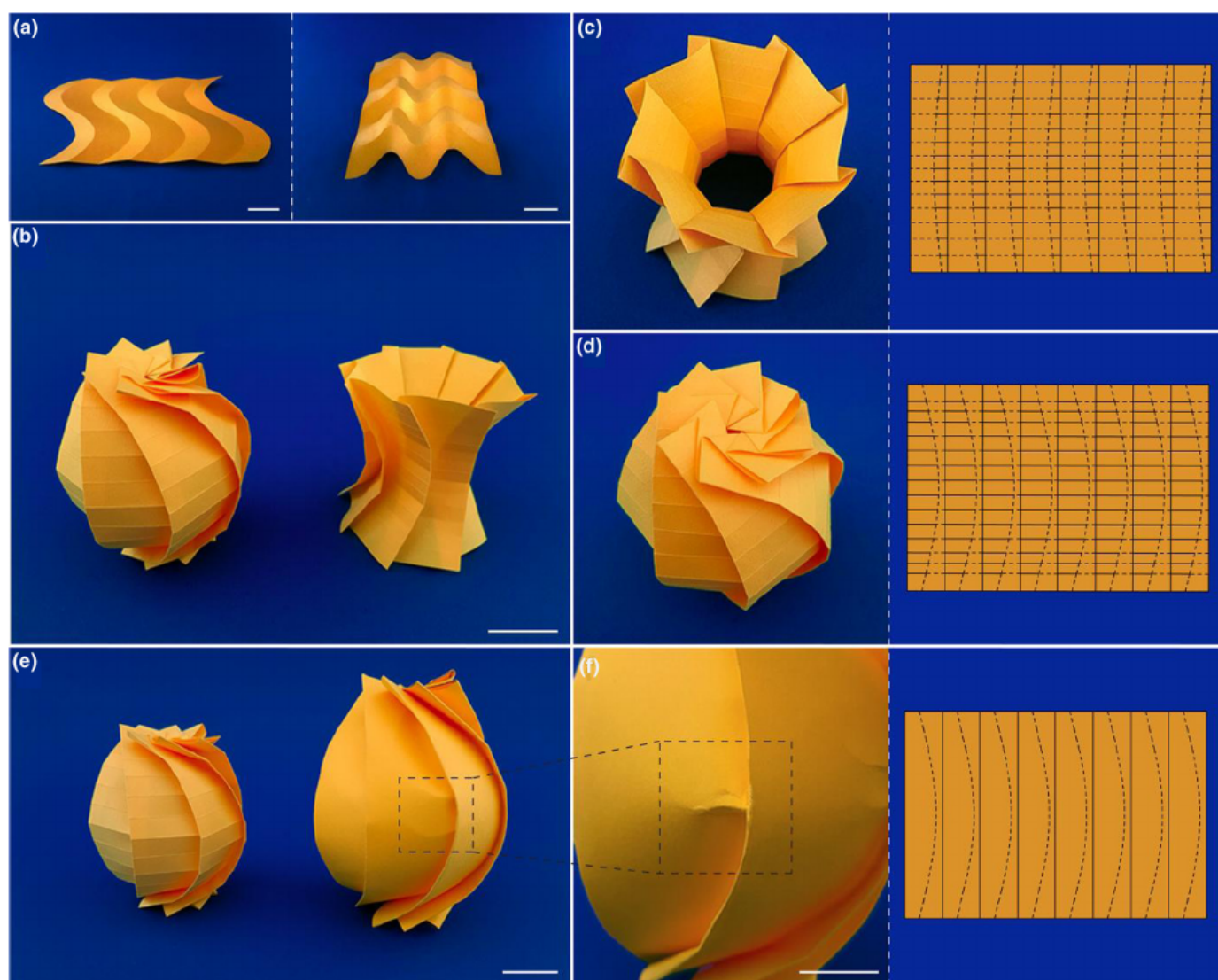
and the bending stiffness of the folded sheet becomes an important parameter [90]. Moreover, the bending induced in the faces necessitates simultaneous folding along multiple creases, complicating automated folding processes [93].

One of the first and most influential analyses of curved creases was performed by Huffman, using Gauss’ spherical representation to examine the local folding behavior [64]. Indeed, the Gauss map of a closed contour crossing a straight-crease maps into a zero-area arc while the map of a contour encompassing a curved crease has non-zero area due to the facet bending, which is indicative of its non-rigid-foldability. The geometry of curved-crease folding has been further explored by Duncan and Duncan [91] and Fuchs and Tabachnikov [94]. They presented several theorems relating the properties of the curved crease to those of the adjacent faces, which are outside the scope of this review. The most important take-away is that folding along a curved crease satisfies the developability of the sheet, meaning that a

curved-folded origami consists of developable patches of either a generalized cylinder, a generalized cone, or a tangent developable to a space-curve [91,95,96]. Hence, folding along curved creases cannot alter the intrinsic curvature of the sheet, as in-plane distortion of the faces occurs. However, curved-crease origami does provide means to alter the *global* intrinsic curvature of flat sheets, in a manner similar to straight-crease folding. More specifically, we identify two approaches to approximate non-zero Gaussian curvature: the use of curved-crease couplets and folding along concentric curved creases. In the current sub-section, only the first approach is discussed, as the latter fits within the broader concept of concentric pleating that is treated in the next sub-section.

Curved-crease couplets, a term introduced by Leong [97], are pairs of curved and straight creases that have been employed by origami artists to create 3D origami with apparent positive and negative intrinsic curvatures. Typically, axisymmetric



**FIGURE 8**

Curved-crease origami. (a) Simple examples of curved-crease origami (Scale bar is 2 cm). (b) An origami sphere (positive Gaussian curvature) and an origami hyperboloid (negative Gaussian curvature) created with the method described by Mitani [98] (Scale bar is 2 cm). (c and d) Top views of the origami hyperboloid and sphere (left panes) and the associated crease patterns (right panes, solid lines are mountain folds and dashed lines are valley folds). (e) Comparison between the standard origami sphere obtained with Mitani's method [98] and the "smooth" variant (Scale bar is 2 cm). (f) Closer view of a wrinkle in the smooth origami sphere, indicative of the frustration between curved and straight creases (left) and the associated crease pattern with horizontal creases (right) (Scale bar is 1 cm).

structures are created from relatively simple crease patterns (Fig. 8). A design method and software tool to generate crease patterns based on "rotational sweep" was proposed by Mitani [98] and a very similar tool was created by Lang [99]. The basic idea is that a flat sheet is "wrapped" around the desired cylindrical or conical geometry and that the excess material is folded into *flaps*, sections of material that are only connected at one edge [100], on the outside surface. This is different from Tachi's origamizing approach [59] in which excess material is tucked away inside the geometry, resulting in more complicated crease patterns [98]. A flap in Mitani's method consists of a kind of curved-crease couplet, containing a straight mountain crease and a piecewise linear valley crease, approximating a curved line. The latter crease represents half of the vertical cross section of the desired shape and, when revolved around the vertical axis, traces out this shape [97,98]. To create the crease pattern, the curved-crease couplets are simply repeated  $N$  times

and arranged on a rectangular sheet (for cylindrical geometries) or on an  $N$ -gon (for conical geometries), with higher values of  $N$  resulting in higher rotational symmetry. Using this method, double-curved shapes could be approximated, as shown in Fig. 8. More recently, Mitani also proposed a variant of this method in which the flaps are replaced by "triangular protrusions" [101]. Again, the excess material that results from wrapping the desired geometry is placed on the outside surface, but this time in a slightly different manner involving four creases instead of two.

Although recent efforts have been made to understand curved-crease origami from a more mathematical perspective [102], it remains a field that is primarily reserved for artists. In such, only limited work has been done that explores the capabilities of curved-crease folding to approximate intrinsically curved surfaces. Nonetheless, it is expected that the use of curved creases has a significant potential in practical origami not only





achieve complex geometries but also for kinetic architectures [96] and shape-programmable structures [103].

### Concentric pleating

As a final category of folding strategies to approximate intrinsically curved surfaces, we consider origami based on concentric pleating, i.e. alternately folding concentric shapes into mountains and valleys. Geometries with apparent negative Gaussian curvature spontaneously result after folding the remarkably simple crease patterns (Fig. 9). The original crease patterns for this origami consisted of equally spaced concentric squares or circles, although variants with ellipses or parabolas have also been folded [90]. One might classify the concentric pleating as a type of origami tessellation, however, we consider it separately due to its remarkable properties.

The classical model with the concentric squares is called the pleated hyperbolic paraboloid or simply *hypar*, after the negatively curved surface it seems to approximate. As explained by Demaine et al., the 3D shape naturally arises due to the paper's physics that balances the tendency of the uncreased paper to remain flat and that of the creased paper to remain folded [104]. Seffen explained the geometry by considering the pleating as a "corrugation strain" toward the center without causing an axial contraction of the hinge lines, thereby forcing the model

to deform out-of-plane [68]. Thus, the pleating introduces a controlled torsion of the flat sheet that is relieved by settling on an energy-minimizing 3D configuration. This principle of anisotropic strain (shrinking) has been recently used by van Manen et al. to program the transformation of flat shape memory polymer sheets into an approximation of a hyper, using thermal activation [105].

Although paper models of the pleated hyper are ubiquitous and well-known among origamists, mathematicians have questioned whether the standard crease pattern of concentric squares could actually result in the pleated hyper. More specifically: does a *proper folding* (folding angles between 0 and  $\pi$ ) along exactly these creases exist? Demaine et al. proved the surprising fact that it does not, hence the folding along the standard crease pattern cannot result in the hyper without some stretching or additional creasing of the paper [104,106]. The problem lies in the twisting of the interior trapezoidal faces of the hyper. While a standard piece of paper could be effortlessly twisted and curled in space, Demaine et al. proved that this twisting should not occur on the interior faces of the hyper. Using aspects of differential geometry, such as the properties of torsal ruled surfaces, the researchers proved two theorems: straight creases must remain straight after folding and a section of the paper bounded by straight creases must remain planar and cannot bend or twist [104].

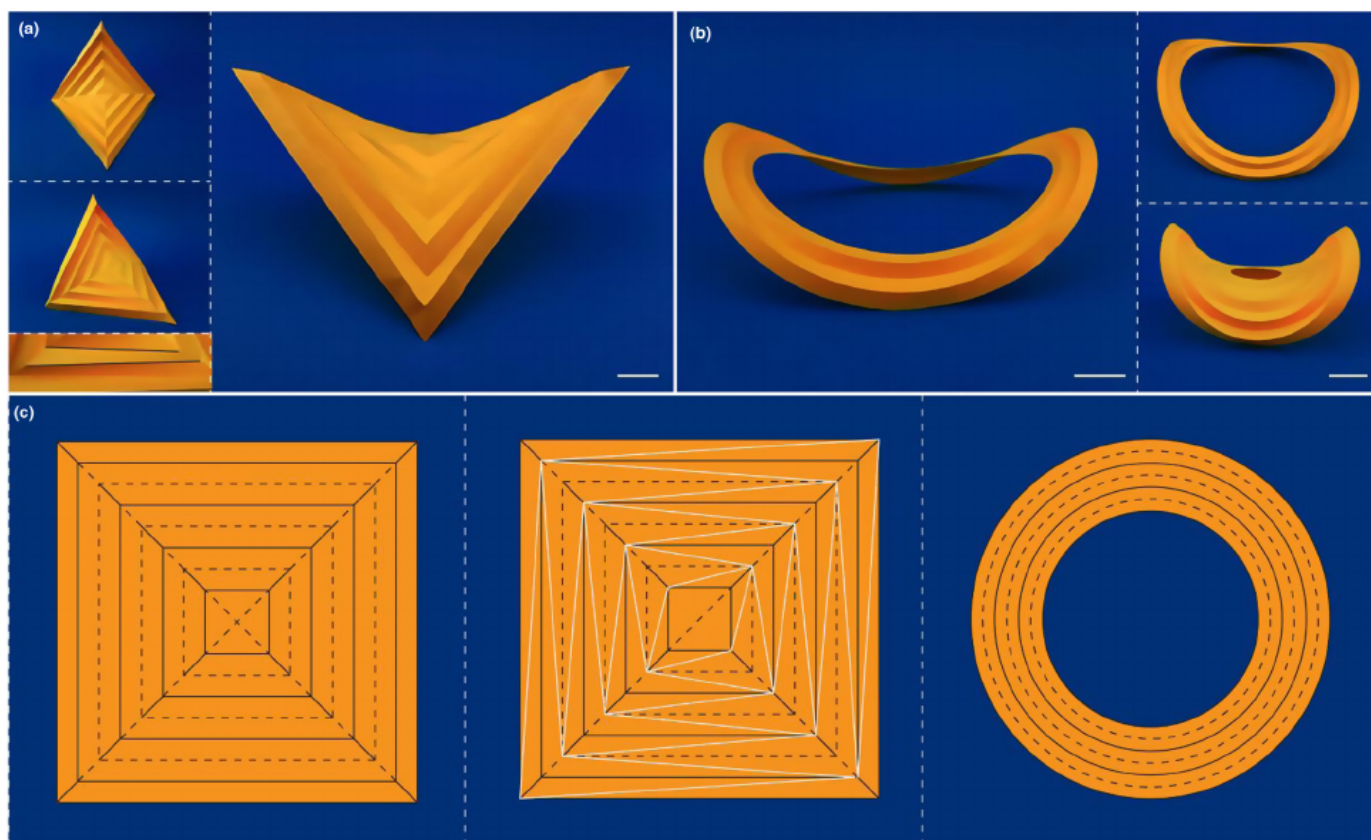


**FIGURE 9**

Concentric pleating origami. (a) Origami hyperbolic paraboloid ("hypar"), obtained by pleating concentric squares. Top left: top view, middle left: side view, bottom left: Closer view of the twisted faces in the standard hyper model, right: side view showing the global saddle-shaped geometry of the hyper (Scale bar is 2 cm). (b) Circular variant of the hyper, obtained by pleating concentric circles (with center hole). Left: side view of an annulus with three creases (Scale bar is 2 cm), top right: top view of an annulus with three creases, bottom right: side view of an annulus with eight creases (Scale bar is 1 cm). (c) Different crease patterns. Left: standard crease pattern for the square hyper, middle: triangulated crease pattern for the square hyper, white lines represent the additional creases that enable proper folding of the hyper (adapted from Ref. [104]), right: crease pattern for the circular hyper (solid lines are mountain folds, dashed lines are valley folds).



Demaine et al. conjecture that the actual folding of the hypar from the standard crease pattern is enabled through additional creases in the paper, potentially many small ones. Alternatively, some stretching at the material level might occur [106]. In any case, it is clear that the folding of the standard crease pattern into the pleated hypar is highly non-rigid, as could also be intuitively understood when drawing a closed curve in one of the square rings: the curve crosses four folds with the same mountain or valley assignment, which cannot fold rigidly according to Gauss' spherical representation [65].

The theorems of Demaine et al. [104] have implications for straight crease origami that exhibits non-rigid behavior, such as the Miura-ori discussed above. It was explained that a (partially) folded Miura-ori could deform out-of-plane through facet bending, which should not be possible according to the above theorems. However, facet bending may be enabled by an additional spontaneous crease in the quadrangular facets, making the facet piecewise planar and satisfying the theorems in doing so. This "triangulation" of the facets has been employed by researchers to capture facet bending in mathematical origami models [69,72,77,107,108]. Moreover, Demaine et al. [104] proved that a triangulation of the standard hypar crease pattern also renders the pattern rigid-foldable, making it possible to create hypars from more rigid materials such as sheet metal [104]. The insights into the hypar crease pattern are also relevant for the curved-crease couplets that were introduced in the previous section, consisting of alternating curved and straight creases. The curved creases require the adjacent faces to bend, while the straight creases do not allow bending. Furthermore, the straight creases do not remain straight in the folded 3D model. Following the theorems of Demaine et al. [104], it thus seems that these curved-crease couplets cannot be folded. This problem is alleviated in Mitani's method [98] by including horizontal creases and representing the curved crease as a piecewise linear crease (Fig. 8c and d), thereby ensuring that the model remains piecewise planar. It must also be noted that the theorems of Demaine et al. [104] are applicable to interior faces (not at the boundary) and fold angles between 0 and  $\pi$ , while the curved-crease couplets end at the paper boundaries and the straight creases seem to be folded at an angle of  $\pi$ . Indeed, Mitani states that the horizontal creases can be omitted when the straight creases are folded close to  $\pi$  [98], resulting in a smooth folded geometry (Fig. 8e). However, closer inspection of such models still reveals the occurrence of small, spontaneous kinks or wrinkles, indicative of the frustration between the straight and curved crease (Fig. 8f).

In addition to the pleated hypar, another classical model is obtained by pleating concentric circles with a hole in the middle (Fig. 9b). Similar to the hypar, this pleated annulus deforms into a saddle, with the degree of curvature depending on the fold angles. Mouthuy et al. attributed this specific deformation to the "overcurvature" of the ring, which is a measure of how much the curvature of the ring exceeds that of a circle with the same circumference [109]. Indeed, the pleating causes the curvature of the concentric creases to increase while their length is preserved, resulting in overcurvature. While Demaine et al. proved that the standard hypar crease pattern cannot be folded without additional creases or stretching, it remains unknown whether

this is also the case for the pleated annulus [104]. However, researchers conjecture that the annulus could be folded following exactly the given crease pattern and that additional creases or stretching are required. Dias et al. investigated the mechanics of the simplest type of pleated annulus: a paper strip with a single circular crease [110]. The researchers provided analytical expressions for the elastic energy of the annulus, to which the faces and the crease contribute. While the incompatibility between the pleating and the resistance to in-plane stretching forces the model to buckle out-of-plane, the actual shape it settles on is determined by the minimization of this elastic energy [110]. Later, Dias and Santangelo extended the work to a pleated annulus with several concentric circles and investigated potential singularities that might arise when attempting to fold the model from the given crease pattern [111]. The researchers did not prove that the crease pattern is exactly foldable, but their results indicated that singularities do not occur for a sufficiently narrow crease spacing, supporting the conjecture of Demaine et al. [104,111].

Concentric pleating is a captivating type of origami, as simple crease patterns result in geometries with apparent intrinsic curvature. Although the mechanisms of this technique are not yet fully understood, particularly for curved creases, concentric pleating could offer an interesting pathway to achieve intrinsic curvature. Especially when extreme values of overcurvature are induced or when different types of hypars or annuli are combined, complex geometries may arise, examples of which are the "hyparhedra" proposed by Demaine et al. [112].

## Kirigami approaches

Kirigami is an art form that is closely related to origami but involves cutting the paper at precise locations. Kirigami has not been explored to the same extent as origami but has recently gained traction among scientists as a promising paradigm for stretchable electronics [38,39,113,114] or advanced honeycomb structures [115–117]. In this section, we review two distinct kirigami approaches that could be employed to approximate intrinsically curved surfaces, namely lattice kirigami and kirigami for engineered elasticity.

### Lattice kirigami

Lattice kirigami is a relatively novel and promising cutting and folding technique that was introduced by Castle et al. [62]. Its essence lies in removing some areas from the sheet through cutting, after which the resulting gaps are closed through folding along prescribed creases. Lattice kirigami has its roots in crystallography, particularly in the defects arising in crystal lattices. Understanding the essentials of this technique therefore requires some terms and concepts from crystallography.

The starting point is the honeycomb lattice, represented by a 2D tessellation of regular hexagons. An infinite flat plane (zero Gaussian curvature) could be tiled using only hexagons, but it is not possible for intrinsically curved surfaces such as spheres or saddles [118]. For example, a soccer ball cannot be tiled with hexagons entirely but requires twelve pentagons to conform to the spherical shape. The insertion of a pentagon or a heptagon within a tiling of hexagons is known as a lattice *disclination*.





which is a type of topological defect that disrupts the orientational order of the lattice [118,119]. These local lattice distortions cause the surfaces to deform out-of-plane to relieve in-plane strains, reminiscent of the metric-driven principles discussed before. The disclinations themselves form concentrated sources of Gaussian curvature: pentagons result in positive Gaussian curvature and heptagons in negative Gaussian curvature [118]. Fig. 10 illustrates the effect of disclinations in a hexagonal weave when a single hexagon is replaced by a pentagon or a heptagon, a technique which has long been employed by basket weavers to create complex shapes [120]. Another type of topological defect is a *dislocation*, which disturbs the translational symmetry of the lattice and is formed by a dipole of disclinations (with opposite topological charge) [118,119]. While disclinations and dislocations are considered defects in a topological sense, they are often necessary distortions of the crystal lattice in natural processes. For example, Sadoc et al. showed that these defects are crucial elements in phyllotaxis, the efficient packing algorithm that nature uses in self-organizing growth processes, such as the spiral distribution of florets in flowers [119,121]. The work of Sadoc et al. [119] was in fact a direct inspiration for Castle et al. to develop lattice kirigami [62].

The basic idea behind lattice kirigami is to strategically remove areas from a honeycomb lattice, paste the newly formed edges together and fold along prescribed creases to create disclination dipoles, resulting in a stepped 3D surface with local concentrations of Gaussian curvature.

Fig. 11a provides a simple example showing two disclination dipoles at the ends of a cut [62]. Inspection of a single disclination dipole reveals that the cutting and pasting transforms one hexagon into a pentagon (by removing a wedge of  $\pi/3$ ) and combines two partial hexagons into a heptagon (i.e. adding a wedge of  $\pi/3$ ), see also Fig. 11c. By systematically exploring cutting and pasting on the honeycomb and its *dual lattice*, Castle et al. established the basic rules for lattice kirigami that satisfy a no-stretching condition and preserve edge lengths on the lattices [62]. The researchers identified the basic units of lattice kirigami: i.e. a 5–7 disclination pair and a 2–4 disclination pair, with the values indicating the coordination number of the vertices (Fig. 11c and d). The gaps that are left after cutting are closed through “climb” or “glide” moves, or a combination of both, in order to result in a stepped surface (Fig. 11a–d). Additionally, the researchers investigated the “sixon” (Fig. 11e), which is obtained by removing an entire hexagon from the honeycomb and closing the gaps using appropriate mountain and valley folds in the adjacent hexagons. Through their basic rules, Castle et al. [62] constructed the foundations for an elegant and new approach toward stepped approximations of freeform surfaces.

Sussman et al. built upon these foundations and demonstrated that lattice kirigami is well-suited to obtain stepped

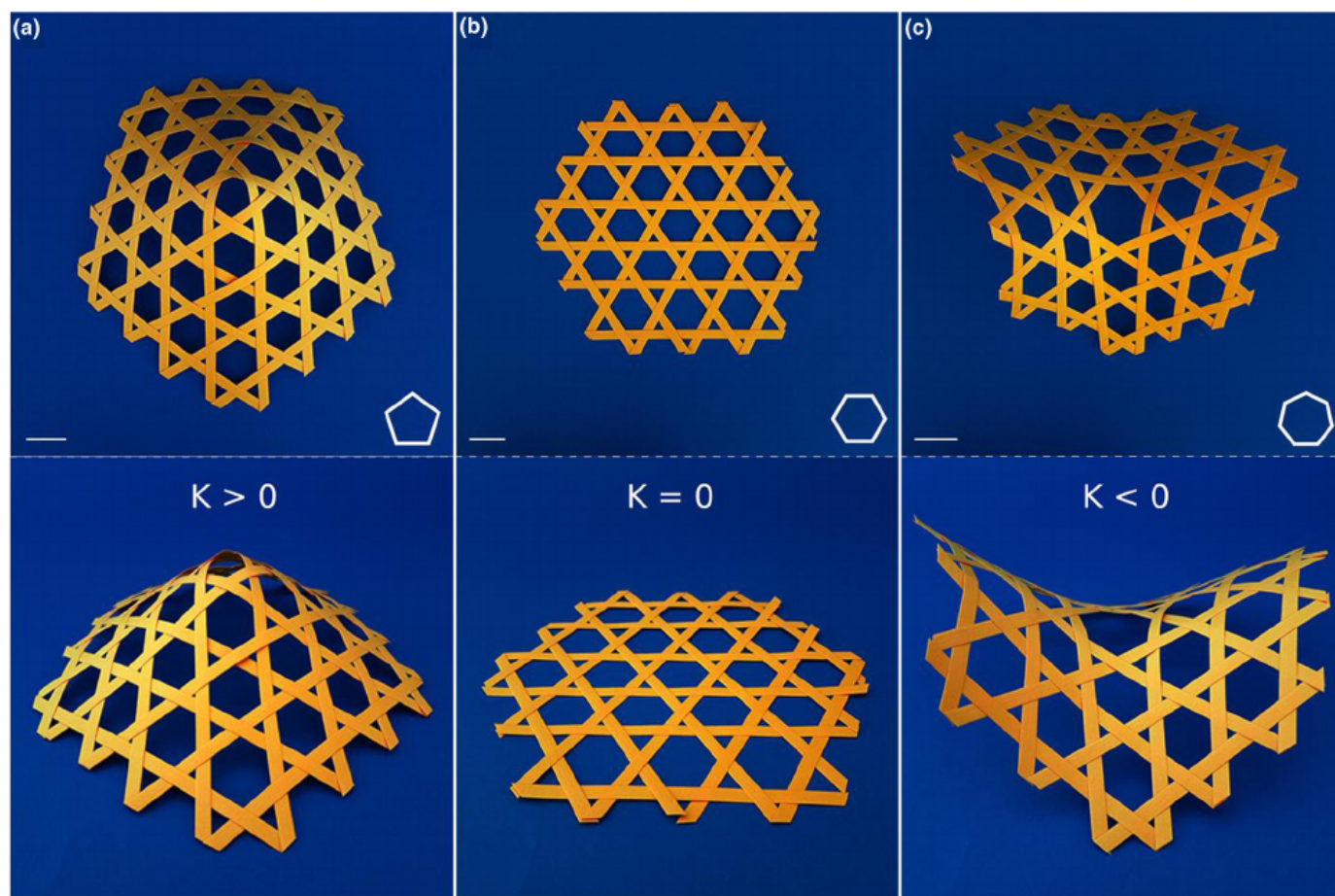
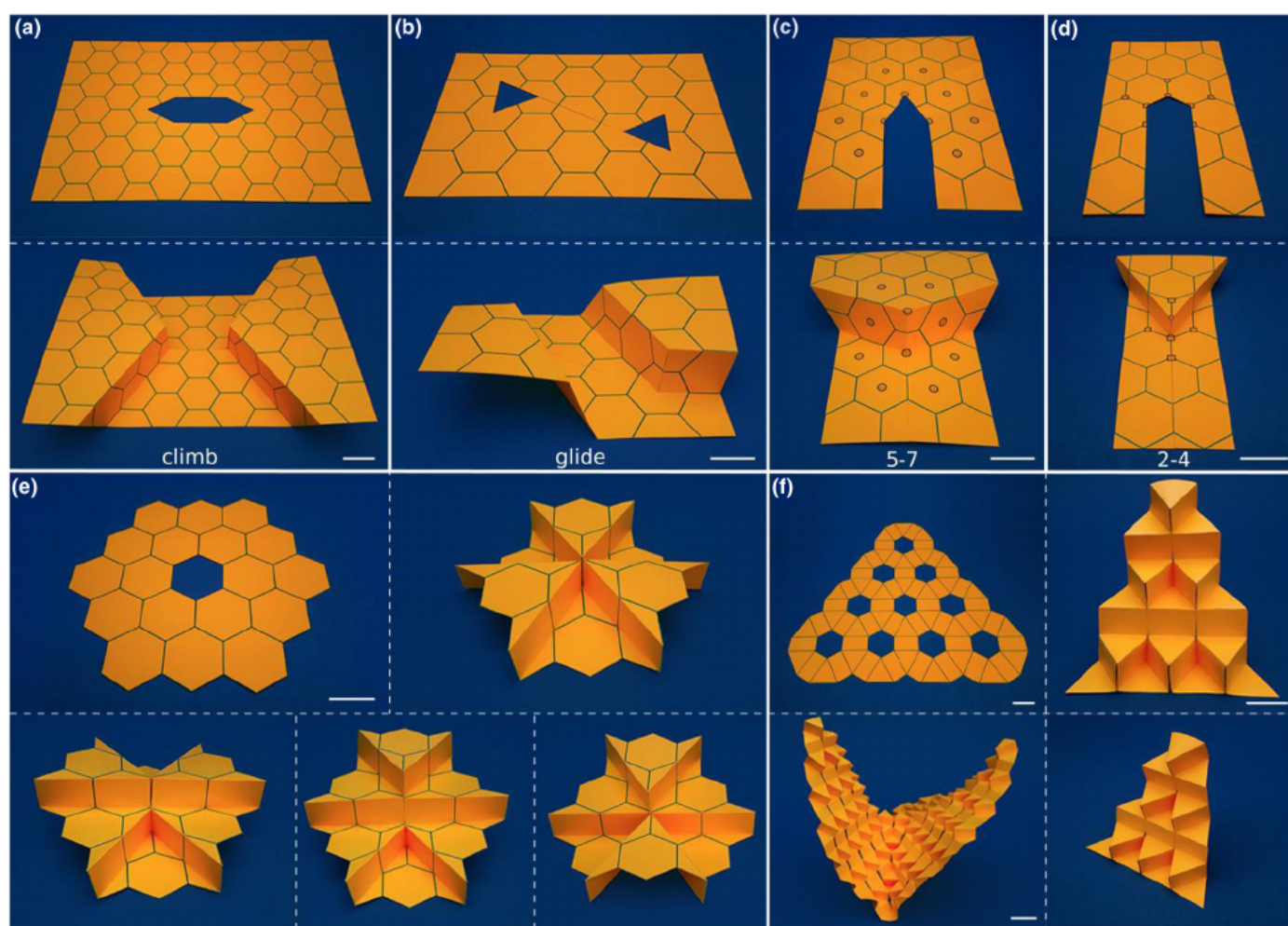


FIGURE 10

Lattice disclinations in a hexagonal lattice. (a) Inserting a single pentagon in a hexagonal weave induces positive Gaussian curvature (Scale bars are 2 cm). (b) A hexagonal weave without lattice disclinations remains flat. (c) Inserting a single heptagon in the hexagonal weave induces negative Gaussian curvature. The physical models photographed were made based on the work presented in Ref. [120].



**FIGURE 11**

Lattice kirigami. (a) The basic principle of lattice kirigami: a wedge is removed from a honeycomb lattice (top), the edges are brought together and the paper is folded along prescribed fold lines (known as a “climb” move). (b) Another basic move, the “glide”, in which the gaps are closed through folding and stitching along the slit connecting the two excised triangles. (c) A “5–7” disclination dipole, characterized by one vertex surrounded by five hexagon centers and another vertex surrounded by seven hexagon centers (represented with the solid circles). (d) A “2–4” disclination dipole; one vertex has two neighboring hexagon corners, the other vertex has four neighboring corners (solid squares). (e) Excising an entire hexagon results in a “sixon”, which could be folded into different configurations by popping the plateaus up or down. (f) Folding a pluripotent “sixon sheet”, i.e. a tessellation of sixons on a triangular lattice, enables stepwise approximations of curved surfaces (e.g. left bottom pane). All scale bars are 2 cm.

approximations of arbitrarily curved surfaces, using a relatively simple inverse design algorithm [122]. Key to their approach is that the kirigami motifs presented by Castle et al. [62] could be folded into several configurations by “popping” the plateaus up or down (Fig. 11e). By connecting many of these motifs together in admissible configurations and properly assigning the plateau heights, complex stepped structures could be obtained. Sussman et al. first considered the use of standard 5–7 climb pairs, but this approach has the important limitation that every target structure requires a new fold and cut pattern [122]. In order to obtain a truly *pluripotent* kirigami pattern that could fit several target shapes, the researchers used sixon motifs. These sixons could be conveniently arranged on a triangular lattice with the centers of the excised hexagons on the lattice points (Fig. 11f). The hexagonal gaps are then closed by folding the remaining hexagons in either one of their allowed configurations (i.e. popping the plateaus upward or downward). As a consequence, a myriad of stepped surfaces could be achieved from this basic kirigami tessellations, simply by varying the mountain/

valley assignment of the fold lines while making sure adjacent plateaus only differ by one sidewall height (i.e. one unit at a time), as shown in Fig. 11f for a saddle-like geometry [122]. The mountain/valley assignment for every fold line could be easily determined from a “height map” of the target surface. Sussman et al. showed that surfaces with arbitrary curvature could be approximated, provided that the gradient with which the surface rises or falls is not too steep (depending on the ratio of plateau width to plateau height). Their results showed that lattice kirigami constitutes a very versatile approach to approximating intrinsically curved surfaces, and has great potential for self-folding due to its simplicity as compared to conventional origami techniques [122].

The most recent progress into lattice kirigami has been made by Castle et al. [123] who generalized their earlier work by removing some of the initially imposed rules and restrictions. Namely, their generalizations included the removal of larger wedges from the sheet and cutting and folding along different angles than the original method. Additionally, the researchers demonstrated





lattice kirigami on other Bravais lattices and arbitrarily complex lattices with a basis [123]. However, the most extensive generalizations came in the form of area-preserving kirigami, in which only slits are made and no material is removed, and additive kirigami, in which new material is actually inserted in the slits, reminiscent of natural growth of cells. Furthermore, Castle et al. showed that complex cuts could be decomposed into the general basic kirigami operations they presented [123]. The researchers envision that the generalized lattice kirigami framework provides more opportunities to create arbitrary shapes from initially flat sheets than the original method, due to the increased freedom in distributing local sources of Gaussian curvature along the sheet. However, a drawback is that the generalizations are not yet suitable with inverse design algorithms, which inhibits the use of such kirigami techniques in practical applications [123].

Lattice kirigami has not received the same attention as traditional origami by the scientific community, the great steps undertaken by the abovementioned researchers notwithstanding. However, it is clear that lattice kirigami offers an exciting and promising paradigm toward 3D structures. By strategically removing material or creating incisions, this technique could alleviate some of the traditional origami issues such as interlocking folds or the cumbersome tucking of excess material (which is non-existent in kirigami), thereby offering higher design freedom and simplicity [62,122,124].

### Kirigami-engineered elasticity

The second kirigami technique we consider here involves cutting the paper at many locations without folding it afterward. The basic idea is that specific cut patterns imbue flat sheets with a high “apparent” elasticity, or stretchability, which does not arise from stretching the actual material but rather from the geometric changes enabled by the cuts, which is why we term this technique *kirigami-engineered elasticity* [39]. Owing to the high stretchability and the scale-independent nature, this technique has recently been proposed as an interesting avenue toward stretchable electronic devices [38,39], small-scale force sensors [113], macro-scale sun-shading [125], and solar-tracking photovoltaics [114]. However, the kirigami-engineered elasticity technique is also useful for wrapping flat sheets on intrinsically curved surfaces since the cuts allow the sheet to locally stretch in-plane, thereby permitting the required metric distortions to conform to the curved surfaces.

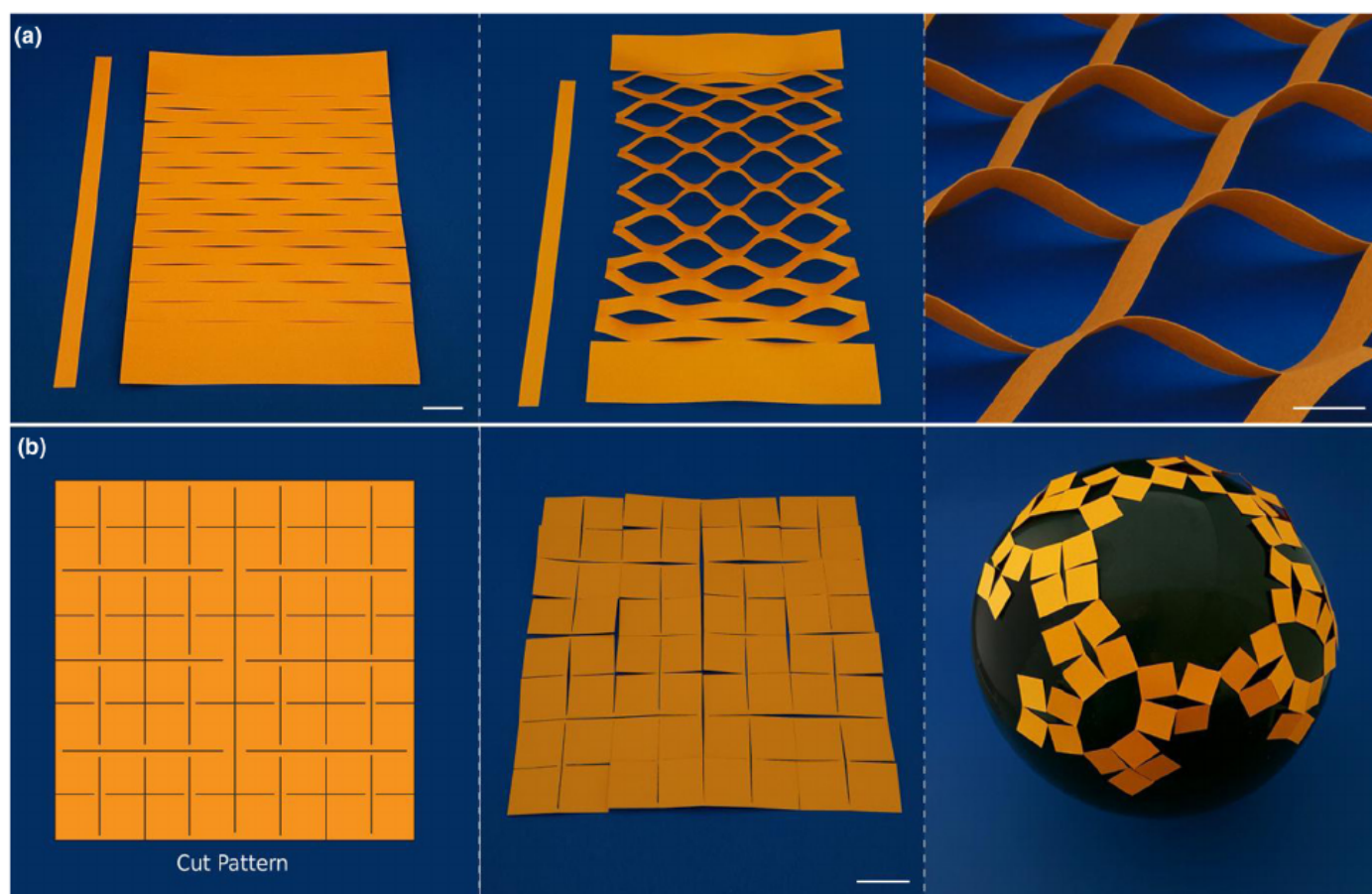
We distinguish two approaches toward kirigami-engineering elasticity in the available literature, one involving out-of-plane buckling of cut struts and one involving in-plane rotation of polygonal units, as shown in Fig. 12 for standard paper models. The former approach involving the out-of-plane buckling was first used by Shyu et al. to create highly stretchable nanocomposite sheets with predictable deformation mechanics [39]. The researchers enriched the nanocomposite sheets with a cut pattern consisting of straight slits in a rectangular arrangement such as the one shown in Fig. 12a. Upon tensile loading perpendicular to the slits, the struts formed by the cutting operation buckle out-of-plane, allowing the overall sheet to reach an ultimate strain of almost two orders of magnitude higher than that of the pristine material (from 4% to 370%) [39]. Around the same time, Blees et al. demonstrated that the same technique is applicable to graphene since this one-atom-thick material behaves similar to

paper in terms of the Föppl–von Kármán number, a measure for the ratio of in-plane stiffness to out-of-plane bending stiffness [113]. Although Fig. 12a shows the struts buckling all in the same direction, this is not necessarily the case and struts might randomly buckle upward or downward, resulting in unpredictable and non-uniform stretching behavior. In order to control a program the tilting of the struts in the desired direction, Tang et al. recently introduced “kiri-kirigami” in which additional notches are etched into the material between the cuts [125]. Those notches are geometrical imperfections in the context of buckling and serve as cues to guide the tilting in the desired direction. By implementing the appropriate notch pattern, the tilting orientation of the struts could be programmed beforehand, and could be varied throughout the same kirigami sheet [125]. All of the abovementioned works used the kirigami technique solely for imparting greater elasticity to flat sheets. However, the out-of-plane buckling that this kirigami technique entails could also be used to efficiently create textured metamaterials from flat sheets, as was recently demonstrated by Rafsanjani and Bertoldi [126]. These researchers perforated thin sheets with a square tiling of orthogonal cuts with a varying orientation with respect to the loading direction. Uniaxial tensile loading results in out-of-plane buckling of the square units, and this could be made permanent by increasing the load beyond the plastic limit of the hinges between the squares. The results are textured “metasheets” which are flat-foldable and could show similar deformation characteristics as Miura-ori sheets, such as negative Gaussian curvature upon non-planar bending [126].

The second method to achieve kirigami-engineered elasticity involves in-plane rotation rather than out-of-plane buckling. In this approach, the imposed cut pattern divides the sheet into (typically square or triangular) units connected through small “hinges” (Fig. 12b). Upon stretching the sheet, the units rotate (almost) freely around the hinges, resulting in a deformation that is driven mostly by the rigid unit rotation instead of stretching the units themselves. Cho et al. used this principle and developed a “fractal” kirigami technique in which the sheet is hierarchically subdivided into ever smaller units that could rotate and contribute to the overall extension of the sheet (Fig. 12c) [40,127]. While an increased level of hierarchy (i.e. more subdivisions) could increase the expandability, there is a limit which is dictated by the allowable rotations of the units. Cho et al. showed that the maximum expandability may be increased by alternating the cut motif between levels, allowing larger rotation angles for the individual units [40]. The researchers demonstrated the fractal kirigami technique at different length scales and achieved an areal expandability of up to 800%. Furthermore, they showed that the kirigami sheets could conform to an object of non-zero Gaussian curvature (a sphere in this case) through non-uniform stretching of the pattern [40], as also shown in Fig. 12b. Further research into fractal kirigami was aimed at understanding the complex mechanics of the hinges, prone to stress concentrations, as well as the influence of material properties [128]. Based on experiments and numerical simulations, Tang et al. proposed dog bone-shaped cuts and hinge widths that vary with the hierarchy level in order to increase the strength and ultimate expandability of the fractal cut patterns (even when applied to brittle materials) [128]. Despite the impress-





**FIGURE 12**

Kirigami-engineered elasticity. (a) A parallel arrangement of slits (left) causes the small struts in between to buckle out of the plane upon tensile load (middle), thereby providing the sheet with higher elasticity (Scale bar is 2 cm). Right: a closer view showing the struts buckling in the same direction (Scale bar is 1 cm). (b) Fractal cut kirigami. Left: a three-level cut pattern with motif alternation, according to Ref. [40]. The small amount of material between adjacent cuts serves as hinge between the rigid square units. Middle: the cut pattern applied to a standard piece of paper (Scale bar is 2 cm). Right: the cut sheet of paper shows a high degree of expandability and could conform to a spherical geometry through rotation of the square units.

expandability that could be achieved with these standard cut patterns, a drawback impeding the adoption in real applications was the lack of compressibility. Therefore, Tang and Yin recently proposed to extend the standard cut pattern, consisting of only slits with actual cut-outs [129]. By introducing circular pores in the original square units, sheet compressibility could be obtained through buckling of the pore walls, while stretchability was still guaranteed by the straight cuts [129].

Comparing the two kirigami-engineered elasticity approaches discussed above, it seems that the fractal cut method is currently more suitable to conform to intrinsically curved surfaces, as it allows biaxial stretching and compression. A drawback of both approaches is that a full coverage of the target surface cannot be achieved, as the stretching is enabled through significant “opening up” of the material. Nonetheless, both methods are expected to receive considerable attention in future research, not only in the field of stretchable electronics but also as a pathway toward mechanical metamaterials. For example, the fractal kirigami patterns are very similar to earlier work on rotation-based auxetic mechanical metamaterials [130,131].

## Discussion and conclusions

We reviewed current origami and kirigami techniques that could be used to approximate or conform to intrinsically curved sur-

faces. Starting off with some concepts from differential geometry, we highlighted the inherent difficulty of transforming flat sheets into intrinsically curved surfaces. Moreover, we explained the geometry of origami, which involves isometric deformation of developable surfaces and therefore retains the intrinsic flatness of the starting material. While scientific research into origami and kirigami is still in its infancy, we could nonetheless identify several promising techniques for the transformation of flat sheets into curved geometries.

### Approximations of intrinsically curved surfaces

The origami and kirigami techniques that we have reviewed could essentially approximate intrinsically curved surfaces in two different ways. One approach is to use origami and kirigami to transform ordinary flat sheets into “metasheets” with significantly altered properties, which are then deformed into the desired geometry. In a second approach, the prescribed fold and cut patterns directly correspond to the final 3D shape and no additional deformation is required after folding. The kirigami-engineered elasticity techniques [39,40,113,125,128,129] are examples of the first approach, while the techniques with tucking molecules [59,81] and curved-crease couplets [97,98,101] are examples of the second. Some techniques could be classified in both categories. For example, origami tessellations could be employed to texture sheets



that they may be deformed into an intrinsically curved geometry [28,68,72,106], but (generalized) tessellations have also been calculated to fit a target surface once folded [73–77]. The lattice kirigami technique may be considered an example of the second approach, as the target shape is programmed into the flat sheet using appropriate cuts and folds. However, a pluripotent version of lattice kirigami has been also proposed [122], in which the same kirigami pattern could be folded to fit multiple curved surfaces.

Due to the developability constraint, no origami or kirigami technique can *exactly* fit a flat sheet onto an intrinsically curved smooth surface. Such surfaces could be approximated in a “global” sense, but locally the folded sheets remain intrinsically flat. Some techniques, such as lattice kirigami [62,122,123] or the origamizing technique [59,88] do imbue the sheets with Gaussian curvature, but this curvature remains concentrated in single points surrounded by developable patches, i.e. “non-Euclidean vertices” [10]. Even when a sheet of paper is crumpled, the majority of the paper remains developable and non-zero Gaussian curvature only arises at specific points due to local stretching of the paper [55,132]. However, owing to the different underlying mechanisms, some techniques will result in a “smoother” approximation of the target surface than others. This is an important factor to consider in applications where the surface topography plays a role, e.g. in fluid flow over an object. Surfaces approximated using origami tessellations or periodic pleating exhibit a textured surface topography. For the periodic pleating technique, this texture is in the form of sharp, parallel ridges. In the case of origami tessellations, the texture is determined by the specific unit cell geometry, with the square waterbomb or Ron Resch patterns resulting in a smoother surface than the Miura-ori pattern, for example. The axisymmetric geometries created by the curved-crease couplets could result in a relatively smooth surface due to the bent faces, although the frustration between the curved and straight creases might entail additional creases that disturb this smoothness. The smoothest approximation of the target surface is likely obtained with the origamizing technique, as the calculated crease pattern (almost) exactly folds into a polygon mesh of this surface. Naturally, a finer mesh results in a smoother representation, yet also entails a more complex folding process. The lattice kirigami technique results in a stepped surface approximation, consisting of many small units that simulate the convex and concave curvatures of the sheet. Interestingly, both the origamizing and lattice kirigami techniques bear strong similarities with computer graphics techniques used to represent 3D objects, either using polygonization of the surface or by means of a “voxel” (volume pixel) representation. Finally, the fractal kirigami technique allows conforming initially flat sheets, made from relatively rigid materials, to surfaces of non-zero Gaussian curvature through non-uniform opening of the cut pattern [40]. However, it was also mentioned that this opening of the perforations inhibits a full coverage of the target surface, which might be a drawback in certain applications.

### Practical considerations

There are several practical challenges that need to be overcome in order to accelerate the adoption of origami and kirigami as a

shape-shifting technique for development of advanced materials. First and foremost is the challenge of the folding itself, which is a labor-intensive manual process in traditional origami. Although all the macroscale paper models that we have presented in this review could be folded by hand, such manual folding becomes increasingly complex at much smaller or much larger scales and for more advanced materials [14,133]. As a consequence, self-folding (i.e. “hands-free” [11]) techniques are required. A wide range of such techniques have been developed during the recent years, in particular aimed at smaller length scales [9–13–16,105,134–142]. While these techniques, for example, differ in terms of materials used, speed, actuation method, and suitability at different length scales, the underlying principle is typically the same: the self-folding behavior is programmed into the flat starting material, most often in the form of “active hinges” which are triggered by an external stimulus to activate folding. In many cases, stimuli-responsive polymeric materials have been employed for this purpose. Examples are hydrogels that swell or de-swell upon a change in aqueous environment [11,141,142], or shape memory polymers (SMP) that shrink when heated above the glass transition temperature [9,105,137–140]. Especially the use of thermally responsive SMP for self-folding has attracted the interest of many researchers due to its simplicity and versatility in terms of actuation method [138], for example via uniform oven heating [122,137], localized joule heating [9], or localized heating by light or microwave absorption [138,139]. The shape memory effect is not limited to polymers but is also present in certain metallic alloys (giving rise to shape memory alloys (SMA)), making these materials also suitable for thermally activated self-folding origami [134]. In addition to these more common techniques, many other actuation methods for self-folding have been developed such as the folding of rigid panels driven by surface tension [143–145] or cell traction forces [136] to create nanoscale and microscale origami, and mechanically driven origami/kirigami [146,147] approaches in which folding is achieved through controlled buckling at specified locations. The reader interested in more detailed information on self-folding techniques and the associated materials is referred to other excellent reviews on these topics [11,14,16,133,148,149].

Despite many recent developments, self-folding remains a challenging task, in part, because of the need for sequential folding and control over the direction of folding and fold angles [9,11,150]. While many of these challenges have been addressed in recent years [9,15,138,150–153], self-folding origami demonstrations have often been restricted to single folds or basic polyhedral shapes [16,138–140,144], while demonstrations of more complicated patterns such as origami tessellations are not so common [137,152]. Given these inherent complexities, it is not surprising that some of the reviewed origami and kirigami techniques are better suited for self-folding than others. Compared to straight creases, self-folding of curved-crease origami is expected to be more challenging despite some recent demonstrations [153]. The facet bending, which is inherent in this type of non-rigid origami, would necessitate larger hinge actuation forces than for purely rigid origami with straight creases. Moreover, the possibility of arriving at a “locked” state during folding may further complicate the automated folding of curved-crease origami [93]. Comparing the tucking molecules origami





technique and the lattice kirigami technique, it has been argued that the latter is more applicable to self-folding [62,122,123]. The tucking molecules approach requires excessive material to be tucked away behind the outer surface, which is a cumbersome process involving many small (crimp) folds and high folding angles. This is in sharp contrast with the lattice kirigami technique, where no excessive material needs to be tucked away and a simple, repetitive folding pattern is used [122]. Indeed, self-folding of basic lattice kirigami units (millimeter and centimeter scale) has been recently demonstrated using localized heating [153] or controlled compressive buckling [146,154], but more complex 3D geometries have not yet been reported. Regarding the techniques that employ the “metasheet” approach, such as the origami tessellations and the kirigami-engineered elasticity, one could argue that these are less suited for self-folding as the sheets need to be actively deformed into the desired shape. In order for these sheets to self-fold into the target geometry, local control over the fold angles or gap opening would be required. Preliminary results show that the standard kirigami cut pattern, consisting of parallel straight cuts, could be actuated using thermally activated local shrinkage [125], but more investigations are needed for metasheets to automatically fit curved surfaces through remotely actuated opening or closing of folds and cuts.

In addition to the self-folding process, another practical consideration is related to locking the origami and kirigami structures in their curved folded geometries. This has, for example, been achieved by annealing titanium-rich origami structures at high temperatures [155]. Another approach is using sequential self-folding to include self-locking mechanisms [149,156]. Alternatively, the locking mechanisms might be inherent to the used origami or kirigami technique. For example, the origamizing technique with tucking molecules uses crimp folds to keep the tucks closed and maintain the desired shape on the outside surface [59]. On the contrary, the standard lattice kirigami cannot benefit from such excess material to lock the folds, although recent generalizations of lattice kirigami enable this to a certain extent by retaining some material for use as “fastening tabs” [123].

In addition to aspects such as self-folding and locking, another prominent challenge is related to the medium to which origami and kirigami are applied. Origami and kirigami are often considered to be scale-independent processes on zero-thickness surfaces. The thin paper sheets that have traditionally been used in these art forms are not too far from zero-thickness surfaces [157]. However, in engineering and scientific applications, the thickness of the flat starting materials cannot be ignored, especially not for applications where the ratio of the sheet thickness to other sheet dimensions is substantial. An important consequence of finite sheet thickness is that appropriate hinge design is required to enable obstruction-free folding and flat-foldability [158]. In recent years, several hinge design approaches to account for finite material thickness have been proposed for rigid-foldable origami [158–160]. In addition to hindering flat-foldability, the material thickness also affects the fold regions themselves, i.e. when the materials are actually folded and the folds are not replaced by hinges. Origami design methods typically assume perfectly sharp folds applied to the (zero-

thickness) sheets, meaning that all folding is concentrated at a single line of infinitesimal width (such a sharp fold is considered to be “ $G^0$  continuous”) [133,161]. While such ideal sharp folds could be approximated to some extent in a thin paper sheet, a fold in a finite thickness sheet will never be perfectly sharp but will rather be defined by some bent region with a certain radius of curvature, especially when thicker materials are used [133,161]. Peraza et al., inspired by Tachi’s origami approach, recently developed an origami design method based on “smooth” folds [161], which are bent surface regions of finite width. Such “smooth” folds form the connection between rigid origami faces and are characterized by higher order geometric continuity than the sharp folds. Smooth folds are not only relevant for folding of thicker materials but also relevant for self-folding techniques based on “active hinges” [161]. Swelling or shrinking at these hinge locations also results in finite regions of bending rather than perfectly sharp folds [162]. This distinction between folds in idealized origami (zero-thickness sheets) and folds in origami on real materials (non-zero-thickness sheet) essentially revolves around the subtle difference between bending and folding [11,157]. Lauff et al. described bending (i.e. smooth fold) as “distributed curvature” while folding as “localized curvature”. However, Liu et al. correctly stated that an overlap between bending and folding exists as it is difficult to draw a clear boundary between localized and distributed curvature [11]. Note that in this context, the term “curvature” refers to single or extrinsic curvature. Bending and folding both result in zero Gaussian (intrinsic) curvature, see Fig. 1 [157].

In light of the techniques reviewed in this paper, origami with finite material thickness is expected to be particularly challenging in the tucking molecules approach, due to many small folds (which are considered to be sharp folds in the origamizer software) and the requirement for flatfolding to tuck away excessive material. As mentioned before, improvements to the standard tucking molecules approach have been proposed to make this technique more apt to real applications with finite thickness materials [81,89,161]. The approach based on the curved-crimp couplets is limited by the fact that very high folding angles (close to  $\pi$ ) are required, which could be difficult to realize with thin materials. The techniques based on origami tessellations, concentric pleating, and lattice kirigami are expected to be better suited for origami with finite thickness sheets as they are generally characterized by simple fold patterns and have already been (self-) folded from materials other than paper [122,152,153,158,162]. Finally, the kirigami-engineered elasticity techniques do not require folding, hence they do not suffer from challenges with tight folds or flat-foldability. Nevertheless, the sheet thickness does influence the load at which out-of-plane buckling of the struts occurs (see Fig. 12a), thereby making it an important design parameter [39,125].

Besides the thickness, another aspect that is often neglected in “idealized” origami is the mechanical properties of the materials, which may also hinder practical application of the origami and kirigami techniques [162]. For example, permanently folding a finite thickness sheet entails a complex stress state involving plasticity and some degrees of stretching, aspects which





strongly linked to the mechanical properties of the sheet [55,104]. Furthermore, non-rigid origami also involves facet bending [90], which is strongly tied to the bending stiffness of the sheets that are used. As for the kirigami-engineered elasticity techniques, it has been already mentioned that these techniques are characterized by high stress concentrations, both for the out-of-plane buckling and in-plane rotation approaches [39,40,125,128]. Consequently, implementation of these techniques to real materials will require certain levels of understanding regarding the local material behavior under these high stress states [128]. Some techniques might therefore be more suitable than others for a given application depending on the chosen material.

As is clear from the preceding discussion, scientific and engineering origami/kirigami are not purely “scale-independent” processes that could be treated solely from a geometrical perspective. For example, self-folding techniques that are suitable for micro-scale origami are not necessarily suitable for architectural-scale origami (e.g. surface tension or cell traction forces). As a final remark, we note that traditional paper seems to remain an excellent medium for origami and kirigami, considering its balance of relative thickness, bending and tearing resistance, and the ability to withstand relatively sharp creases. However, this does not necessarily mean that other materials (on different scales) are less well suited as these materials might behave very similar to paper when used for origami or kirigami [113].

## Outlook

Approximating intrinsically curved surfaces using origami and kirigami is relevant for many applications that can benefit from the specific advantages offered by these techniques: the ability to obtain complex geometries from (nearly) non-stretchable flat sheets and the ability to apply this on virtually any length scale. As such, the folding-and-cutting paradigm could enable the development of flexible electronics [38,40], shape-morphing materials [122], nano- and microscale devices [14,163], architectural structures [84,159], or any other complex geometry involving intrinsic curvature. The applications of origami and kirigami are not limited to static designs, but could also be of a more dynamic nature. In fact, certain fold patterns involving facet bending or curved creases may form energetic barriers between different folding states, giving rise to bi-stability and fast snapping motions that could be leveraged for switchable or tunable devices [103,164].

Interesting opportunities for origami and kirigami may be also found in the rapidly expanding field of biomedical engineering [36], with such examples as patterned micro-containers for controlled drug delivery [35], origami stent grafts [34], or self-folding tetherless micro-grippers [165]. A particularly interesting bio-application is the folding of 3D tissue scaffolds from flat sheets enriched with cell-regulating surface topographies. Self-folding of patterned scaffolds with simple geometries has already been demonstrated [166], but more complex curved geometries would be needed in order to better stimulate and guide tissue regeneration [167]. For example, it has been hypothesized that promising bone-mimicking scaffolds could be based on triply periodic minimal surfaces (TPMS) [168,169]. These are area-minimizing 3D

surfaces with zero mean curvature ( $H$ ) everywhere, corresponding to negative (or zero) Gaussian curvature everywhere ( $H = \frac{1}{2}(\kappa_1 + \kappa_2) = 0$  and thus  $\kappa_1 = -\kappa_2$ ) [42]. These intrinsically curved minimal surfaces are ubiquitous in biological systems [41,170–172] and are nature’s best attempt at dealing with the frustration of embedding constant negatively curved surfaces in Euclidean 3-space (Hilbert’s theorem) [173,174]. Current TPMS scaffolds are created with additive manufacturing [4,169], meaning that the surface topographies needed to enhance tissue regeneration cannot be included. However, the origami and kirigami techniques we have reviewed here might enable transforming patterned flat sheets into intrinsically curved scaffolds through appropriate cutting and folding.

In conclusion, we have reviewed recent work on origami and kirigami to identify the techniques that enable shape shifting of flat sheets into complex geometries. By introducing aspects from differential geometry, in particular the Gaussian curvature, we have illustrated the fundamental difference between flat sheets and intrinsically curved surfaces, which can explain going from wrapping of spheres to wavy edges in plant leaves. While plane distortions could imbue the flat sheets with intrinsic curvature, we have shown that origami and kirigami offer alternative approaches to *approximate* curved surfaces with (almost) no stretching of the underlying material. Despite originating from centuries-old art forms, the techniques we have reviewed here are promising for many applications across a broad range of length scales. It could therefore be expected that the relatively recent interest in “scientific” origami and kirigami will only keep on growing in the near future.

## Acknowledgments

This research has received funding from the European Research Council under the ERC grant agreement n° [677575].

## References

- [1] A.A. Zadpoor, J. Malda, *Ann. Biomed. Eng.* 45 (1) (2017) 1–11.
- [2] M. Kadic et al., *Appl. Phys. Lett.* 100 (19) (2012) 191901.
- [3] R. Hedayati, A.M. Leeftang, A.A. Zadpoor, *Appl. Phys. Lett.* 110 (9) (2017) 091905.
- [4] F.S.L. Bobbert et al., *Acta Biomater.* 53 (2017) 572–584.
- [5] E.B. Duoss et al., *Adv. Funct. Mater.* 24 (31) (2014) 4905–4913.
- [6] T. Jiang, Z. Guo, W. Liu, *J. Mater. Chem. A* 3 (5) (2015) 1811–1827.
- [7] O.Y. Loh, H.D. Espinosa, *Nat. Nanotech.* 7 (5) (2012) 283–295.
- [8] S. Dobbenga, L.E. Fratila-Apachitei, A.A. Zadpoor, *Acta Biomater.* 46 (2016) 14.
- [9] S.M. Felton et al., *Soft Matter* 9 (32) (2013) 7688–7694.
- [10] C.D. Santangelo, *Annu. Rev. Condens. Matter Phys.* 8 (1) (2016).
- [11] Y. Liu, J. Genzer, M.D. Dickey, *Prog. Polym. Sci.* 52 (2016) 79–106.
- [12] R. Guseinov, E. Miguel, B. Bickel, *ACM Trans. Graph.* 36 (4) (2017) 1–12.
- [13] A.M. Hubbard et al., *Soft Matter* 13 (12) (2017) 2299–2308.
- [14] J. Rogers et al., *MRS Bull.* 41 (02) (2016) 123–129.
- [15] N. Bassik, G.M. Stern, D.H. Gracias, *Appl. Phys. Lett.* 95 (9) (2009) 91901.
- [16] T.G. Leong, A.M. Zafarshar, D.H. Gracias, *Small* 6 (7) (2010) 792–806.
- [17] M.Z. Li et al., *J. Mater. Process. Technol.* 129 (2002) 333–338.
- [18] T. Gutowski et al., *Compos. Manuf.* 2 (1991) 147–152.
- [19] Y. Klein, E. Efrati, E. Sharon, *Science* 315 (5815) (2007) 1116–1120.
- [20] A.S. Gladman et al., *Nat. Mater.* 15 (4) (2016) 413–418.
- [21] J. Kim et al., *Science* 335 (6073) (2012) 1201–1205.
- [22] E. Sharon, M. Marder, H.L. Swinney, *Am. Sci.* 92 (2004) 254–261.
- [23] E. Sharon et al., *Nature* 419 (2002) 579.
- [24] H. Liang, L. Mahadevan, *Proc. Natl. Acad. Sci. USA* 108 (14) (2011) 5516–5521.
- [25] K. Miura, *Inst. Space Astronaut. Sci. Rep.* 618 (1985) 1–9.



- [26] Guest, S.D., Pellegrino, S., Inextensional wrapping of flat membranes, in: Motro, R., Wester, T. (eds.), *First Int. Sem. on Struct. Morph.*, Montpellier, 1992, pp 203–215.
- [27] S.A. Zirbel et al., *J. Mech. Des.* 135 (11) (2013) 111005.
- [28] M. Schenk, S.D. Guest, *Proc. Natl. Acad. Sci. USA* 110 (9) (2013) 3276–3281.
- [29] E.T. Filipov, T. Tachi, G.H. Paulino, *Proc. Natl. Acad. Sci. USA* 112 (40) (2015) 12321–12326.
- [30] J.L. Silverberg et al., *Science* 345 (6197) (2014) 647–650.
- [31] J.T. Overvelde et al., *Nature* 541 (7637) (2017) 347–352.
- [32] M. Eidini, G.H. Paulino, *Sci. Adv.* 1 (2015) 8.
- [33] S. Felton et al., *Science* 345 (6197) (2014) 644–646.
- [34] K. Kuribayashi et al., *Mater. Sci. Eng. A* 419 (1–2) (2006) 131–137.
- [35] C.L. Randall et al., *Adv. Drug. Deliv. Rev.* 59 (15) (2007) 1547–1561.
- [36] C.L. Randall, E. Gultepe, D.H. Gracias, *Trends Biotechnol.* 30 (3) (2012) 138–146.
- [37] R.J. Lang, *Phys. World* 20 (2) (2007) 30.
- [38] Z. Song et al., *Sci. Rep.* 5 (2015) 10988.
- [39] T.C. Shyu et al., *Nat. Mater.* 14 (8) (2015) 785–789.
- [40] Y. Cho et al., *Proc. Natl. Acad. Sci. USA* 111 (49) (2014) 17390–17395.
- [41] S. Hyde et al., *The Language of Shape: The Role of Curvature in Condensed Matter: Physics, Chemistry and Biology*, Elsevier Science, Amsterdam, The Netherlands, 1996.
- [42] D. Hilbert, S. Cohn-Vossen, *Geometry and The Imagination*, Chelsea Publishing Company, New York, USA, 1990.
- [43] J.R. Weeks, *The Shape of Space*, CRC Press, Boca Raton, FL, USA, 2001.
- [44] C.R. Calladine, *Theory of Shell Structures*, Cambridge University Press, Cambridge, UK, 1983.
- [45] V.A. Toponogov, V. Rovenski, *Differential Geometry of Curves and Surfaces: A Concise Guide*, Birkhäuser Boston, New York, NY, USA, 2005.
- [46] V. Rovenski, *Modeling of Curves and Surfaces with MATLAB*, Springer Science & Business Media, New York, NY, USA, 2010.
- [47] M. Spivak, *A Comprehensive Introduction to Differential Geometry*, vol. II, Publish or Perish, Inc., Houston, Texas, USA, 1990.
- [48] B. O'Neill, *Elementary Differential Geometry*, Academic Press (Elsevier), Burlington, MA, USA, 2006.
- [49] E. Sharon, E. Efrati, *Soft Matter* 6 (22) (2010) 5693.
- [50] M. Marder, R.D. Deegan, E. Sharon, *Phys. Today* 60 (2) (2007) 33–38.
- [51] R.D. Kamien, *Science* 315 (2007) 1083–1084.
- [52] A.N. Pressley, *Elementary Differential Geometry*, Springer Science & Business Media, Dordrecht, The Netherlands, 2010.
- [53] E. Efrati et al., *Phys. D* 235 (1–2) (2007) 29–32.
- [54] H. Aharoni, E. Sharon, R. Kupferman, *Phys. Rev. Lett.* 113 (25) (2014) 257801.
- [55] T.A. Witten, *Rev. Mod. Phys.* 79 (2) (2007) 643–675.
- [56] E. Efrati, E. Sharon, R. Kupferman, *J. Mech. Phys. Solids* 57 (4) (2009) 762–775.
- [57] E. Demaine, M. Demaine, Recent results in computational origami, in: T. Hull (Ed.), *Origami 3: Proceedings of the 3rd International Meeting of Origami Science, Math, and Education (OSME 2001)*, A K Peters/CRC Press, Boca Raton, FL, USA, 2002, pp. 3–16.
- [58] E.D. Demaine, M.L. Demaine, J.S.B. Mitchell, *Comput. Geom.* 16 (1) (2000) 3–21.
- [59] T. Tachi, *IEEE Trans. Vis. Comput. Graphics* 16 (2) (2010) 298–311.
- [60] Z. Abel et al., *J. Comput. Geom.* 7 (2016) 171–184.
- [61] T.A. Evans et al., *R. Soc. Open Sci.* 2 (9) (2015) 150067.
- [62] T. Castle et al., *Phys. Rev. Lett.* 113 (24) (2014) 245502.
- [63] Miura, K., A note on intrinsic geometry of origami, in: Huzita, H., (ed.), *First Int. Meeting of Origami Science and Technology*, Ferrara, Italy, 1989, pp 239–249.
- [64] D.A. Huffman, *IEEE Trans. Comput.* C-25 (10) (1976) 1010–1019.
- [65] T. Hull, *Project origami: activities for exploring mathematics*, second ed., CRC Press, Boca Raton, FL, USA, 2012.
- [66] R.C. Alperin, B. Hayes, R.J. Lang, *Math. Intell.* 34 (2) (2012) 38–49.
- [67] E. Gjerde, *Origami Tessellations Awe-Inspiring Geometric Designs*, A K Peters/CRC Press, Boca Raton, FL, USA, 2008.
- [68] K.A. Seffen, *Philos. Trans. A Math. Phys. Eng. Sci.* 370 (1965) (2012) 2010–2026.
- [69] A.A. Evans, J.L. Silverberg, C.D. Santangelo, *Phys. Rev. E Stat. Nonlin. Soft Matter Phys.* 92 (1) (2015) 013205.
- [70] L. Mahadevan, S. Rica, *Science* 307 (2005).
- [71] C. Lv et al., *Sci. Rep.* 4 (2014) 5979.
- [72] M. Schenk, S.D. Guest, Origami folding: A structural engineering approach, in: P. Wang-Iverson et al. (Eds.), *Origami 5: Fifth International Meeting of Origami Science, Mathematics, and Education (SOSME)*, A K Peters/CRC Press, Boca Raton, FL, 2011, pp. 291–304.
- [73] T. Tachi, *J. Int. Assoc. Shell Spatial Struct.* 50 (3) (2009) 173–179.
- [74] J.M. Gattas, W. Wu, Z. You, *J. Mech. Des.* 135 (11) (2013) 111011–111016.
- [75] P. Sareh, S.D. Guest, *Int. J. Space Struct.* 30 (2) (2015) 141–152.
- [76] F. Wang, H. Gong, X. Chen, C.Q. Chen, *Sci. Rep.* 6 (2016) 33312.
- [77] L.H. Dudte, E. Vouga, T. Tachi, L. Mahadevan, *Nat. Mater.* 15 (5) (2016) 588.
- [78] Y. Chen et al., *Proc. R. Soc. A* 472 (2190) (2016) 20150846.
- [79] R.D. Resch, *The Topological Design of Sculptural and Architectural Systems*, Nat. Comp. Conf. and Exp., ACM, New York, 1973, pp. 643–650.
- [80] Resch, R.D., Christiansen, H., The design and analysis of kinematic folded systems, in: *IASS Symp. on Folded Plates and Prism. Struct.*, Vienna, 1973.
- [81] T. Tachi, *J. Mech. Des.* 135 (2013) 111006.
- [82] T. Tachi, Rigid folding of periodic origami tessellations, in: K. Miura et al. (Eds.), *Origami 6: Mathematics*, American Mathematical Society, Providence, RI, USA, 2016.
- [83] H. Nassar, A. Lebee, L. Monasse, *Proc. R. Soc. A* 473 (2197) (2016) 20160001.
- [84] T. Tachi, *J. Geom. Graph.* 14 (2) (2010) 203–215.
- [85] X. Zhou, H. Wang, Z. You, *Proc. R. Soc. A* 471 (2181) (2015) 20150407.
- [86] K. Song et al., *Proc. R. Soc. A* 473 (2200) (2017) 20170016.
- [87] Lang, R.J., A computational algorithm for origami design, in: *Twelfth Int. Symp. on Comput. Geom.*, Philadelphia, 1996.
- [88] Tachi, T., 3D origami design based on tucking molecules, in: Lang, R. J., *Origami 4, Proceedings of 4OSME: 4th International Conference on Origami in Science, Mathematics and Education*, A K Peters/CRC Press, Boca Raton, FL, USA, 2009, pp 259–272.
- [89] Demaine, E., Tachi, T., Origamizer: a practical algorithm for folding polyhedron, in: Aronov, B., and Katz, M. J., (eds.), *33rd Int. Symp. on Comput. Geom. (SoCG 2017)*, Schloss Dagstuhl–Leibniz-Zentrum fuer Informatik, Dagstuhl, Germany, 2017.
- [90] E.D. Demaine et al., *Symm. Cult. Sci.* 26 (2) (2015) 145–161.
- [91] J.P. Duncan, J.L. Duncan, *Proc. R. Soc. A* 383 (1784) (1982) 191–205.
- [92] Geretschläger, R., Folding curves, in: Lang, R. J., (ed.), *Origami 4, Proceedings of 4OSME: 4th International Conference on Origami in Science, Mathematics and Education*, A K Peters/CRC Press, Boca Raton, FL, USA, (2009), pp 151–163.
- [93] M. Kilian, A. Monszpart, N.J. Mitra, *ACM Trans. Graph.* 36 (3) (2017) 1–12.
- [94] D. Fuchs, S. Tabachnikov, *Am. Math. Month.* 106 (1999) 27–35.
- [95] M. Kilian et al., *ACM Trans. Graph.* 27 (2008) 75.
- [96] A. Vergauwen, L.D. Laet, N.D. Temmerman, *Comput. Aided Des.* 83 (2017) 63.
- [97] Leong, C. C., Simulation of nonzero gaussian curvature in origami by crease couplets, in: Lang, R. J., (ed.), *Origami 4, Proceedings of 4OSME: 4th International Conference on Origami in Science, Mathematics and Education*, A.K. Peters/CRC Press, Boca Raton, FL, USA, 2009, pp 151–163.
- [98] J. Mitani, *Comput. Aided Des. Appl.* 6 (1) (2009) 69–79.
- [99] Lang, R. J., Origami Flanged Pots, <http://demonstrations.wolfram.com/OrigamiFlangedPots/>, in: *Wolfram Demonstrations Project*, vol. 2017.
- [100] R.J. Lang, *Origami Design Secrets: Mathematical Methods for an Ancient Art*, second ed., A K Peters/CRC Press, Boca Raton, FL, USA, 2011.
- [101] J. Mitani, A design method for axisymmetric curved origami with triangular prism protrusions, in: P. Wang-Iverson et al. (Eds.), *Origami 5: Proceedings of the 5th International Meeting of Origami Science, Mathematics, and Education (SOSME)*, A K Peters/CRC Press, Boca Raton, FL, 2011, pp. 437–447.
- [102] E.D. Demaine et al., Characterization of curved creases and rulings design analysis of lens tessellations, in: K. Miura et al. (Eds.), *Origami 6: Mathematics*, American Mathematical Society, Providence, RI, USA, 2016, pp. 209–230.
- [103] N.P. Bende et al., *Proc. Natl. Acad. Sci. USA* 112 (36) (2015) 11175–11180.
- [104] E.D. Demaine, M.L. Demaine, V. Hart, G.N. Price, T. Tachi, *Graphs Combin.* 27 (3) (2011) 377–397.
- [105] T. van Manen, S. Janbaz, A.A. Zadpoor, *Mater. Horiz.* (2017), <https://doi.org/10.1039/C7MH00269F>.
- [106] M. Schenk, *Folded Shell Structures* (Ph.D. thesis), University of Cambridge, 2011.
- [107] Tachi, T., Simulation of rigid origami, in: Lang, R. J., (ed.), *Origami 4, Proceedings of 4OSME: 4th International Conference on Origami in Science, Mathematics and Education*, A K Peters/CRC Press, Boca Raton, FL, USA, 2009, pp 151–163.
- [108] Z.Y. Wei et al., *Phys. Rev. Lett.* 110 (21) (2013) 215501.
- [109] P.O. Mouthuy et al., *Nat. Commun.* 3 (2012) 1290.
- [110] M.A. Dias et al., *Phys. Rev. Lett.* 109 (11) (2012) 114301.
- [111] M.A. Dias, C.D. Santangelo, *EPL (Europhys. Lett.)* 100 (5) (2012) 54005.
- [112] Demaine, E. D., Demaine, M. L., Lubiw, A., Polyhedral sculptures of hyperbolic paraboloids, in: *2nd Ann. Conf. of BRIDGES: Mathematics Connections in Art, Music, and Science*, Kansas, USA, 1999.
- [113] M.K. Blees et al., *Nature* 524 (7564) (2015) 204–207.



- [114] A. Lamoureux et al., *Nat. Commun.* 6 (2015) 8092.
- [115] R.M. Neville, F. Scarpa, A. Pirrera, *Sci. Rep.* 6 (2016) 31067.
- [116] K. Saito, F. Agnese, F. Scarpa, *J. Intell. Mater. Syst. Struct.* 22 (9) (2011) 935–944.
- [117] S. Del Broccolo, S. Laurenzi, F. Scarpa, *Compos. Struct.* 176 (2017) 433–441.
- [118] W.T. Irvine, V. Vitelli, P.M. Chaikin, *Nature* 468 (7326) (2010) 947–951.
- [119] J.F. Sadoc, N. Rivier, J. Charvolin, *Acta Crystallogr. Sect. A: Found. Crystallogr.* 68 (4) (2012) 470–483.
- [120] Martin, A.G., A basketmaker's approach to structural morphology, in: *Int. Assoc. Shell Spatial Struct. (IASS) Symp.*, Amsterdam, The Netherlands, 2015.
- [121] J. Charvolin, J.-F. Sadoc, *Biophys. Rev. Lett.* 06 (01n02) (2011) 13–27.
- [122] D.M. Sussman et al., *Proc. Natl. Acad. Sci. USA* 112 (24) (2015) 7449–7453.
- [123] T. Castle et al., *Sci. Adv.* 2 (9) (2016) e1601258.
- [124] F. Wang et al., *J. Appl. Mech.* 84 (6) (2017) 061007.
- [125] Y. Tang et al., *Adv. Mater.* 29 (10) (2016) 1604262.
- [126] A. Rafsanjani, K. Bertoldi, *Phys. Rev. Lett.* 118 (8) (2017) 084301.
- [127] S. Yang, I.-S. Choi, R.D. Kamien, *MRS Bull.* 41 (02) (2016) 130–138.
- [128] Y. Tang et al., *Adv. Mater.* 27 (44) (2015) 7181–7190.
- [129] Y. Tang, J. Yin, *Extr. Mech. Lett.* 12 (2017) 77–85.
- [130] R. Gatt et al., *Sci. Rep.* 5 (2015) 8395.
- [131] H.M.A. Kolken, A.A. Zadpoor, *RSC Adv.* 7 (9) (2017) 5111–5129.
- [132] M. Ben Amar, Y. Pomeau, *Proc. R. Soc. A* 453 (1959) (1997) 729–755.
- [133] E.A. Peraza-Hernandez et al., *Smart Mater. Struct.* 23 (9) (2014) 094001.
- [134] E. Hawkes et al., *Proc. Natl. Acad. Sci. USA* 107 (28) (2010) 12441–12445.
- [135] S. Janbaz, R. Hedayati, A.A. Zadpoor, *Mater. Horiz.* 3 (6) (2016) 536–547.
- [136] K. Kuribayashi-Shigetomi, H. Onoe, S. Takeuchi, *PLoS One* 7 (12) (2012) e51085.
- [137] M.T. Tolley et al., *Smart Mater. Struct.* 23 (9) (2014) 094006.
- [138] Y. Liu et al., *Soft Matter* 8 (6) (2012) 1764–1769.
- [139] D. Davis et al., *RSC Adv.* 5 (108) (2015) 89254–89261.
- [140] D. Davis et al., *J. Mech. Robot.* 8 (3) (2016) 031014.
- [141] J. Guan et al., *J. Phys. Chem. B* 109 (49) (2005) 23134–23137.
- [142] G. Stoychev, N. Puretskiy, L. Ionov, *Soft Matter* 7 (7) (2011) 3277–3279.
- [143] B. Gimi et al., *Biomed. Microdevices* 7 (4) (2005) 341–345.
- [144] A. Azam et al., *Biomed. Microdevices* 13 (1) (2011) 51–58.
- [145] D.H. Gracias et al., *Adv. Mater.* 14 (3) (2002) 235.
- [146] Z. Yan et al., *Adv. Funct. Mater.* 26 (16) (2016) 2629–2639.
- [147] Y. Zhang et al., *Proc. Natl. Acad. Sci. USA* 112 (38) (2015) 11757–11764.
- [148] Y. Zhang et al., *Nat. Rev. Mater.* 2 (4) (2017) 17019.
- [149] T. Van Manen, S. Janbaz, A.A. Zadpoor, *Mater. Today* 21 (2) (2018) 144–150.
- [150] T. Tachi, T.C. Hull, *J. Mech. Robot.* 9 (2) (2017). 021008-021008-021009.
- [151] Y. Liu, B. Shaw, M.D. Dickey, J. Genzer, *Sci. Adv.* 3 (2017) 3.
- [152] J.H. Na et al., *Adv. Mater.* 27 (1) (2015) 79–85.
- [153] Q. Zhang et al., *Extr. Mech. Lett.* 11 (2017) 111–120.
- [154] Y. Shi et al., *Extr. Mech. Lett.* 11 (2017) 105–110.
- [155] B.Y. Ahn, D. Shoji, C.J. Hansen, et al., *Adv. Mater.* 22 (20) (2010) 2251–2255.
- [156] Y. Mao et al., *Sci. Rep.* 5 (2015) 13616.
- [157] Lauff, C., et al., Differentiating bending from folding in origami engineered using active materials, in: *Proceedings of the ASME 2014 International Design Engineering Technical Conferences & Computers and Information Technology Engineering Conference*, 2014, p V05BT08A040.
- [158] Y. Chen, R. Peng, Z. You, *Science* 349 (6246) (2015) 396–400.
- [159] T. Tachi, Rigid-foldable thick origami, in: P. Wang-Iverson et al. (Eds.), *Origami 5: Fifth International Meeting of Origami Science, Mathematics, and Education (SOSME)*, A K Peters/CRC Press, Boca Raton, FL, 2011, pp. 253–260.
- [160] R.J. Lang et al., *J. Mech. Robot.* 9 (2) (2017) 021013.
- [161] E.A. Peraza Hernandez, D.J. Hartl, D.C. Lagoudas, *Proc. R. Soc. A* 473 (2222) (2017) 20160716.
- [162] N. An, M. Li, J. Zhou, *Smart Mater. Struct.* 25 (11) (2016) 11LT02.
- [163] L. Xu, T.C. Shyu, N.A. Kotov, *ACS Nano* 11 (2017) 7587–7599.
- [164] J.L. Silverberg, J.H. Na, A.A. Evans, et al., *Nat. Mater.* 14 (4) (2015) 389–393.
- [165] T.G. Leong et al., *Proc. Natl. Acad. Sci. USA* 106 (3) (2009) 703–708.
- [166] M. Jamal et al., *Biomaterials* 31 (7) (2010) 1683–1690.
- [167] A.A. Zadpoor, *Biomater. Sci.* 3 (2) (2015) 231–245.
- [168] S.C. Kapfer et al., *Biomaterials* 32 (29) (2011) 6875–6882.
- [169] S.B. Blanquer et al., *Biofabrication* 9 (2) (2017) 025001.
- [170] K. Michielsen, D.G. Stavenga, J. R. Soc. Interface 5 (18) (2008) 85–94.
- [171] J.W. Galusha et al., *Phys. Rev. E Stat. Nonlin. Soft Matter Phys.* 77 (5 Pt 2) (2008) 050904.
- [172] H. Jinnai et al., *Adv. Mater.* 14 (22) (2002) 1615–1618.
- [173] M.E. Evans, G.E. Schröder-Turk, *Asia Pacific Math. Newsllett.* 5 (2) (2015) 30.
- [174] S.T. Hyde, G.E. Schröder-Turk, *Interface Focus* 2 (2012) 529–538.



